

Rowan University

## Rowan Digital Works

---

Theses and Dissertations

---

7-9-2014

### Investigation of compaction characteristics of subbase material using the superpave gyratory compactor

Craig Kumpel

Follow this and additional works at: <https://rdw.rowan.edu/etd>



Part of the [Civil and Environmental Engineering Commons](#)

**Let us know how access to this document benefits you - share your thoughts on our feedback form.**

---

#### Recommended Citation

Kumpel, Craig, "Investigation of compaction characteristics of subbase material using the superpave gyratory compactor" (2014). *Theses and Dissertations*. 254.

<https://rdw.rowan.edu/etd/254>

This Thesis is brought to you for free and open access by Rowan Digital Works. It has been accepted for inclusion in Theses and Dissertations by an authorized administrator of Rowan Digital Works. For more information, please contact [LibraryTheses@rowan.edu](mailto:LibraryTheses@rowan.edu).

**INVESTIGATION OF COMPACTION  
CHARACTERISTICS OF SUBBASE MATERIAL  
USING THE SUPERPAVE GYRATORY  
COMPACTOR**

by  
Craig Jason Kumpel

A Thesis

Submitted to the  
Department of Civil Engineering  
College of Engineering  
In partial fulfillment of the requirement  
For the degree of  
Master of Science in Civil Engineering  
at  
Rowan University  
December 26, 2013

Thesis Chair: Beena Sukumaran, Ph.D.

© 2013 Craig J Kumpel

## **Acknowledgements**

I wish to thank all those who helped me. Without them, none of this research could have been completed. I would like to thank my advisor, Beena Sukumaran for granting me the opportunity to work on this study. She has bestowed upon me persistent support and confidence throughout the duration of the study necessary to drive me to its completion. It was her encouragement that caused me to push myself harder and to better myself in the process.

I would also like to thank Dr. Mehta for his continuous support throughout the duration of the project and for taking time out of his hectic schedule to provide help and guidance and has provided me with the necessary tools that have led me to become a better engineer. Additionally, I would like to thank Dr. Cleary who has also taken time from his busy schedule to join my committee. His assistance throughout my career at Rowan University has proven invaluable toward becoming a better, well-rounded engineer.

I would like to thank my family and friends who have supported me throughout this project. Without their selfless support, none of this would have been possible. I would like to thank all the undergraduates that have lent a helping hand in the acquisition and analysis of the large amount of data.

I would also like to thank the Federal Aviation Administration for the research grant that made this work possible. In particular, I would like to thank Dr. Gordon Hayhoe, who has since retired, and Dr. David Brill of the FAA for their assistance with the project.

## **Abstract**

Craig Kumpel

### **INVESTIGATION OF COMPACTION CHARACTERISTICS OF SUBBASE MATERIAL USING THE SUPERPAVE GYRATORY COMPACTOR**

2012/13

Beena Sukumaran, Ph.D.

Master of Science in Civil Engineering

The purpose of this study is to complete an in-depth analysis of data from both the Federal Aviation Administration's (FAA) full-scale testing and Superpave Gyratory Compactor testing to determine if the SGC is a valuable tool for the prediction of airport pavement performance and design. The practicality of the SGC was based on extensive laboratory and field testing of three unbound materials including P-154, P-209, and DGA, which are the subbase and base materials used by the FAA at the National Airport Pavement Test Facility (NAPTF). During the past construction cycles at the NAPTF, it has been found that the flexible pavements failed due to excessive compaction of the subbase material. To better study this phenomena in the laboratory, SGC tests were done at various moisture contents, while varying other variables such as the confining pressure and number of gyrations. The laboratory tests were correlated with field performance characteristics during construction such as changes in density of the soil with each pass of the roller. It was found that the SGC results are capable of replicating the field compaction characteristics irrespective of the roller used. In addition, the laboratory SGC results were correlated with field trafficking data such as magnitude of deflections with each pass of the aircraft gear and a direct correlation has been found.

The excessive compaction observed in the subbase layer during trafficking is shown to be due to abrasion and attrition of the aggregate changing the aggregate from an angular to a more rounded aggregate, which reduces interlock and causes more compaction. Ultimately, the study has provided correlations between passes of various landing gear configurations and gyrations in the SGC.

## Table of Contents

Abstract.....	iv
List of Figures.....	ix
List of Tables .....	xi
Chapter 1 - Introduction.....	1
1.1    Background Information.....	1
1.2    Problem Statement.....	2
1.3    Significance of Research.....	4
1.4    Study Objectives .....	4
1.5    Research Approach .....	5
1.5.1    Literature Review.....	5
1.5.2    Data Acquisition .....	6
1.5.3    Results Analysis.....	6
1.5.4    Design Elements and Validation.....	6
1.6    Thesis Structure .....	7
Chapter 2 – Literature Review .....	9
2.1    Airport Pavement Base and Subbase Materials.....	9
2.1.1    P-154 Subbase Material .....	9
2.1.2    P-209 Subbase Material .....	10
2.2    Full Scale Testing .....	10
2.2.1    National Airport Pavement Test Facility (NAPTF) Setup.....	12
2.2.2    Airbus Testing.....	20
2.3    Multi-wheel Multi-gear Configurations.....	22
2.4    Effects of Wander .....	23

## Table of Contents (Continued)

2.5	Compaction.....	25
2.5.1	Field Construction Compaction (Construction) Methods .....	25
2.5.2	Laboratory Compaction .....	26
2.5.3	Compaction Mechanics.....	30
2.6	Laboratory Testing Using the Superpave Gyratory Compactor .....	34
2.6.1	SGC Readouts and Settings .....	35
2.6.2	Pressure Distribution Analyzer for Energy Analysis .....	36
2.6.3	Previous Studies Using the SGC on Soil .....	38
2.7	Testing Goals .....	44
Chapter 3 – Laboratory Testing Results .....		47
3.1	Material Classification and Properties .....	47
3.2	P-154 Laboratory Experiment Results.....	47
3.3	P-209 Laboratory Experiment Results.....	53
3.4	DGA Laboratory Experiment Results.....	59
3.5	SGC Compaction Curve Comparison .....	64
3.6	Energy Measurements.....	66
Chapter 4 – Field to Laboratory Comparison .....		77
4.1	P-154 Field Compaction Results .....	77
4.2	P-154 Evaluation of Performance Characteristics .....	79
4.3	P-209 Field Compaction Results .....	81
4.4	P-209 Evaluation of Performance Characteristics .....	82
Chapter 5 – Conclusions .....		86
5.1	Summary of Findings.....	86



## Table of Contents (Continued)

5.2	Recommendations.....	87
5.3	Future Work.....	88
	List of References .....	89

## List of Figures

FIGURE 2-0-A. AIRBUS A380 LANDING GEAR CONFIGURATION .....	11
FIGURE 2-0-B. BOEING B777 LANDING GEAR CONFIGURATION .....	11
FIGURE 2-0-C. ENCLOSED RUNWAY TEST STRIP WITH TEST VEHICLE .....	13
FIGURE 2-0-D. NORTHSIDE OF CC3 AT 19,500 PASSES.....	14
FIGURE 2-0-E. CUSTOMIZABLE TRUCK IN A SIX-WHEEL CONFIGURATION.....	14
FIGURE 2-0-F. MULTI-DEPTH DEFLECTOMETERS (MDD) BEFORE INSTALLATION .....	15
FIGURE 2-0-G. MDD INSTALLED IN TEST STRIP.....	15
FIGURE 2-0-H. NORMAL DISTRIBUTION CURVE OF WANDER .....	16
FIGURE 2-0-I. CROSS-SECTIONAL TEST SECTION COMPOSITIONS OF CC3.....	17
FIGURE 2-0-J. CROSS-SECTION OF TRAFFICKED LFC-2 TEST ITEM.....	18
FIGURE 2-0-K. CROSS-SECTIONAL TEST SECTION COMPOSITIONS OF CC5 .....	20
FIGURE 2-0-O. COMMON ROLLER TYPES: SMOOTH-WHEELED ROLLER (TOP LEFT), PNEUMATIC RUBBER-TIRED ROLLER (TOP RIGHT), SHEEPSFOOT ROLLER (BOTTOM LEFT), AND THE INTERNAL VIBRATORY ATTACHMENT (BOTTOM RIGHT).....	26
FIGURE 2-0-P. VISUAL DESCRIPTION OF THE PROCTOR TESTS AND A TYPICAL PROCTOR CURVE.....	28
FIGURE 2-0-Q. DIAGRAM OF PROCTOR CURVE.....	28
FIGURE 2-0-R. TROXLER SUPERPAVE GYRATORY COMPACTOR AND ILLUSTRATION OF SAMPLE MOLD OFFSET.....	30
FIGURE 2-0-S. ILLUSTRATION OF AGGREGATE BREAKAGE MODES (A. FRACTURE, B. ATTRITION, AND C. ABRASION) .....	33
FIGURE 2-0-T. PRESSURE DISTRIBUTION ANALYZER (PDA) AND SCHEMATICAL REPRESENTATION, RIGHT ..	37
FIGURE 2-0-U. COMPACTION CURVES FOR A-2-4 SOIL WITH 12% FINES AT VARIOUS GYRATION RATES.....	40
FIGURE 2-0-V. COMPACTION CURVES FOR A-2-4 SOIL AT VARIOUS GYRATION COUNTS .....	41
FIGURE 2-0-W. COMPACTION CURVES FOR A-2-4 SOIL AT VARIED GYRATION ANGLES.....	41
FIGURE 2-0-X. COMPACTION CURVES FOR A-2-4 SOIL AT VARIOUS PRESSURES .....	42

## List of Figures (Continued)

FIGURE 2-0-Y. COMPARISON OF PROCTOR CURVES TO CURVES COMPILED USING SGC DATA.....	43
FIGURE 3-0-A. EVALUATION OF P-154 RESULTS BELOW OMC .....	49
FIGURE 3-0-B. COMPACTION COMPARISON OF 3000G AND 5000G SAMPLES.....	49
FIGURE 3-0-C. P-154 GRADATION ANALYSIS.....	53
FIGURE 3-0-D. EVALUATION OF P-209 RESULTS BELOW OMC .....	55
FIGURE 3-0-E. P-209 GRADATION ANALYSIS.....	56
FIGURE 3-0-F. P-209 FLAT AND ELONGATED ON 9.53MM SIEVE.....	58
FIGURE 3-0-G. P-209 FLAT AND ELONGATED ON 12.7MM SIEVE .....	59
FIGURE 3-0-H. EVALUATION OF DGA SGC RESULTS BELOW OMC .....	60
FIGURE 3-0-I. DGA SIEVE ANALYSIS.....	62
FIGURE 3-0-J. DGA FLAT AND ELONGATED ON 9.53MM SIEVE .....	63
FIGURE 3-0-K. DGA FLAT AND ELONGATED ON 12.7MM SIEVE .....	63
FIGURE 3-0-L. COMPACTION CURVES FOR P-154 AT 2 TO 2.5% MOISTURE CONTENT RANGE.....	65
FIGURE 3-0-M. COMPACTION CURVES FOR P-209 AT 2 TO 2.5% MOISTURE CONTENT RANGE.....	65
FIGURE 3-0-N. COMPACTION CURVES FOR DGA AT 2 TO 2.5% MOISTURE CONTENT RANGE .....	66
FIGURE 3-0-O. P-154 ENERGY MEASUREMENTS .....	68
FIGURE 3-0-P. P-209 ENERGY MEASUREMENTS.....	70
FIGURE 3-0-Q. SUM OF ENERGY MATERIAL COMPARISON FOR P-154 AND P-209.....	71
FIGURE 3-0-R. VERTICAL WORK PER GYRATION AT 2.75% M.C. FOR P-154 AND P-209.....	72
FIGURE 3-0-S. SHEAR WORK PER GYRATION COMPARISON OF P-154 AND P-209 .....	74
FIGURE 4-0-A. P-154 CONSTRUCTION TO SGC DENSITY CORRELATION.....	78
FIGURE 4-0-B. P-154 GRADATION ANALYSIS EVALUATION.....	80
FIGURE 4-0-C. P-209 CONSTRUCTION TO SGC DENSITY CORRELATION.....	81
FIGURE 4-0-D. P-209 GRADATION ANALYSIS EVALUATION.....	83
FIGURE 4-0-E. P-209 FLAT AND ELONGATED ON 9.53MM SIEVE.....	84
FIGURE 4-0-F. P-209 FLAT AND ELONGATED ON 12.7MM SIEVE.....	85

## **List of Tables**

TABLE 3-0-A. FAA P-154, DGA, AND P-209 MATERIAL AND CLASSIFICATION PROPERTIES .....	47
TABLE 3-0-B. P-154 SGC RESULTANT DATA .....	51
TABLE 3-0-C. SGC RESULTS FOR P-209 FIELD COMPACTION COMPARISONS .....	56
TABLE 3-0-D. SGC RESULTS FOR DGA FIELD COMPACTION COMPARISONS .....	61
TABLE 3-0-E. AVERAGE SGC WORK AT 600 kPa TO OBTAIN MODIFIED PROCTOR DENSITY.....	76

# **Chapter 1**

## **Introduction**

### **1.1 Background Information**

Within the past couple of decades, the introduction of larger planes, such as the 1.3-million pound (0.6-million kg) Airbus A380 (Airbus Industrie, 2001), raises concern within the Federal Aviation Administration (FAA) as to the suitability of existing airport pavements for these heavier loads. Consequently, the FAA currently tests airport pavements under heavy aircraft loading at the National Airport Pavement Test Facility (NAPTF) in Atlantic City, NJ, USA. The resulting data from the simulated heavy aircraft loading is leading to the belief that the subbase layer is being compacted past the maximum Modified Proctor Density (ASTM D1557) during the simulated trafficking (Hayhoe and Garg, 2007). In order to better understand the compaction and shear flow characteristics of the subbase layer during construction and trafficking, a Superpave Gyrotory Compactor (SGC) was used to compact the materials at various stress levels and at different moisture contents.

In addition, to thoroughly analyze the compaction characteristics of each of these materials in the SGC, Rowan University is continuously monitoring the performance of the materials throughout the construction phase and simulated trafficking performed at the FAA's full scale testing facility. This data is being collected through the FAA and continues to be assessed in this ongoing study.

## **1.2 Problem Statement**

Full-scale testing, like that being performed at the NAPTF, provides invaluable data as to the effects of continuous loading and trafficking of airport runways and taxiways.

However, this testing is quite expensive and time consuming. Currently, it is assumed during full scale testing that pavement layers are constructed in a manner to prevent significant densification during trafficking. However, resultant data from full scale testing has shown that the modified proctor test is not capable of reaching the realistic upper limit of densities attained during trafficking. The search for a more suitable test than the modified proctor has directed attention to the potential use of the Superpave Gyrotory Compactor (SGC). The primary function of SGC is to test and examine asphalt samples (AASHTO, 2004). Therefore, testing of unbound materials by use of an SGC is a relatively new idea (Mokwa, 2008). Standard testing procedures like the Standard and Modified Proctor methods, ASTM D698 and ASTM D1557, generally define quality control measures for compaction and also what is often considered the maximum theoretical dry densities of soil. However, recent improvements in the capabilities of modern construction equipment and the introduction of heavier airplanes allow for greater compaction and higher densities in the field than seen in the Proctor tests. For this reason there is now a great interest in the possibility of using the SGC to determine optimum moisture content and maximum dry density, as well as the life cycle of these soils in an accelerated manner. The SGC is believed to more closely simulate the actual compaction process during construction and trafficking. The results of SGC testing also provide insight into the mechanisms of compaction and the effects of different variables on the compaction process.

During full scale tests at the NAPTF, significant densification of the subbase layer occurred under aircraft trafficking accompanied by shear flow failure in the low strength, California bearing ratio of less than 3, subgrade material. In order to understand the compaction and shear flow characteristics of the subbase layer during construction and trafficking, the material is compacted in the SGC at various stress levels and moisture contents similar to those being used in the full-scale tests. Since the SGC's primary use is to study compaction of asphalt concrete, the compaction parameters in the SGC are adjusted to closely resemble field compaction of the subbase material during construction at similar moisture contents. This calibration provides the benchmark values for laboratory evaluation of unbound material in the SGC, such as stress level and the angle of gyration. The shape of the compaction curve and the density at various gyration quantities provide an understanding of the compaction characteristics of the subbase material throughout construction and trafficking. Additionally, this study includes testing to obtain actual energy measurements within the SGC during compaction and a correlation of this data with the energy transferred during compaction and trafficking in the field. In addition, the field data from the most recent asphaltic construction cycle, CC5, helps determine the effect of subbase thickness, quality, and compaction on flexible pavement response during trafficking.

The main limitation of this approach is that the stress regime of the subbase in the field is different from the stress regime in the laboratory due to different confining conditions. The assumption remains that this has a small effect on the actual data but is still being considered during analysis.

### **1.3 Significance of Research**

The airport pavement design industry is the main benefactor of this study. Design and analysis tools for flexible pavement design are being developed that are suited to the loads applied by the heavier, modern aircraft. These tools use the compaction results from the SGC to relate to densities seen from trafficking and construction in the field. In this study, the SGC serves as a more suitable tool than the modified proctor due to its ability to better represent the in-situ stress regime induced by a rolling wheel.

Additionally, sample sizes can be varied in size in the SGC which allows the testing of realistic lift heights. This simulates the pavement geometry well and provides greater insight into the field compaction. In addition, through the use of various confining pressures, the various loading cases are being simulated closely.

### **1.4 Study Objectives**

In previous studies completed by Rowan University, it was shown that free water from lifts constructed at optimum moisture content drained into the top layer of the clay subgrade, which reduced the strength. As a result of this Rowan recommended that the FAA reduce moisture content in the P-154 lifts below optimum. Due to the recent success of this recommendation, the study is being expanded to address the following objectives.

- The Superpave Gyratory Compactor's efficiency and suitability as a predictor of field compaction.
- Effects of moisture content and migration of moisture on the densification of the material using the Superpave Gyratory Compactor.



- The change in aggregate performance metrics, such as shape, angularity, and grain-size distribution, after trafficking and compaction in the Superpave Gyratory Compactor.
- The mechanism of compaction during trafficking is investigated using the performance metric data.
- A correlation between construction roller passes and gyrations in the Superpave Gyratory Compactor.

## **1.5 Research Approach**

### **1.5.1 Literature Review**

The literature review includes a detailed look into full scale testing apparatus used to develop design procedures for airport pavements. Also incorporated is an in-depth review of the current uses of the SGC on unbound material. In addition to these two major portions, background information on material properties, multi-wheel/multi-gear configuration, current construction methods and wander are also reviewed. The goals of the literature review are to:

1. Observe certain aspects from the full scale testing critical to this study including the excessive compaction of the subbase layer due to heavy aircraft loading, effects of gear configuration, effects of wander, means of data collection, etc.
2. Evaluate past studies on the SGC including tests conducted on unbound material to better understand the limitations and possibilities of the use of the apparatus.
3. Understand the current construction methods in order to aid with comparisons of SGC data.

### **1.5.2 Data Acquisition**

In the field, data for each layer of the flexible pavement are collected before, during, and after trafficking to determine material properties such as density, moisture content, and gradation. In the lab, data are collected from various pieces of equipment to determine many of the same properties. These tasks along with the information from the literature review provide the basis of the analysis conducted in this study, in which field testing data is compared to laboratory testing results.

### **1.5.3 Results Analysis**

The results of the study are analyzed both qualitatively and quantitatively. SGC testing is compared to modified proctor testing to show its better suitability in a situation such as airport taxiways. SGC testing is also analyzed relative to full scale testing showing its ability to mimic compaction methods and maximum densities. Compaction methods are also analyzed through performance metric testing such as aggregate image analysis, flat and elongated testing, and gradation analyses.

### **1.5.4 Design Elements and Validation**

#### **1.5.4.1 Design**

The information from the literature review, full scale testing and laboratory testing provides all the support necessary to prove the SGC as a viable alternative to the modified proctor as a standard for specifying in-situ densities of airport runway/taxiway subbases and base layers. A general design element is being developed to relate

construction densities and maximum trafficked densities to densities obtainable within the SGC.

#### **1.5.4.2 Validation**

The densities of the SGC are compared against test data available from the FAA.

Compaction data is obtained from sand cone and nuclear density after compaction in the field then is utilized for comparison to SGC densities, given a relatively equivalent amount of compaction. A variety of performance metric tests are employed to verify that the methods of compaction are similar as well.

### **1.6 Thesis Structure**

Within Chapter 2 of this thesis is a comprehensive literature review section. The main focus of Chapter 2 is to provide readers and future researchers with the proper background information to fully understand the subject matter in the study. The section begins with an explanation of the current dilemma with airport pavements as well as current design methods used to deal with their inadequacy. Additionally, it describes the recent findings from full scale testing, effects of wander, multi-wheel multi-gear configurations, construction compaction, and the Superpave Gyratory Compactor. The literature review section holds the information necessary to freshen up on or learn specific aspects of compaction mechanics, tools of pavement design, etc.

Following the literature review section are the results of the study and an extensive analysis of those results in Chapter 3. Chapter 3 includes crucial information from which

to draw conclusions. The conclusions are discussed in Chapter 4 as well as recommendations developed from them. A final section in Chapter 5 is included to summarize further studies that are being performed as an extension upon this study.

## **Chapter 2**

### **Literature Review**

#### **2.1 Airport Pavement Base and Subbase Materials**

Subbase and Base layers of airport pavements typically consist of materials specified by the FAA. The materials discussed in these studies include P-154 and P209. The material specifications can be found in FAA Advisory Circular 150/5370-10F (FAA 150/5370-10F, 2011). These specifications discuss the gradation, construction methods, and other material properties for each material. This section summarizes the information given by the specifications for the P-154 and P-209.

##### **2.1.1 P-154 Subbase Material**

This material contains granular aggregate of high hardness and durability. The material should be a blend consisting of fine sand, clay, stone dust, or an equivalent approved materials. The blend shall have a uniform gradation and have the potential to be compacted into a very dense and stable state. The material shall not have organic matter, excessive amounts of clay, or other foreign particles.

This subbase course should be placed and compacted in layers. No layer shall be less than 75 mm and no more than 200 mm after compaction is complete. The material should not be spread more than 1,700 sq. m prior to rolling. The field compaction of the material should be considered complete when the density is 100 percent of the maximum modified proctor density. Density in the field should be measured using either ASTM D 1556 or ASTM D 6938. Further soil characteristics for P-154 are shown in Chapter 3.

### **2.1.2 P-209 Subbase Material**

This material should contain clean crushed stone, crushed gravel, or crushed slag aggregate of high durability. The fine aggregate in the mixture shall be fines from the mechanical crushing of the coarse particles. However, the addition of other fine aggregate is allowed if necessary to create the correct gradation. The blend shall not contain coatings of clay, silt, vegetable matter, and other foreign materials including clay balls.

This base course should be placed using a mechanical spreader onto a moistened subgrade. It should be placed in uniform layers with a maximum compacted thickness of 150 mm. Compaction should take place immediately after spreading has been completed. Field density should be 100 percent of maximum modified proctor upon completion of the compaction operations. Density should be measured on a lot basis and sampling locations must be determined using the methods prescribed in ASTM D 3665 (Date). Densities shall be determined using either ASTM D 1556 or ASTM D 6938. Further soil characteristics for P-209 are shown in Chapter 3.

## **2.2 Full Scale Testing**

Within recent years, the growth in commercial passenger flights continues to increase demand for larger and heavier aircrafts with greater capacity. Consequently, companies, such as Boeing and Airbus, continually introduce larger aircraft like the B777 and the A380, respectively. As the aircraft grow in size, the landing gears grow proportionately in complexity; examples of current aircraft landing gear can be seen in Figure 2-0-a and

Figure 2-0-b. This complex landing gear places a higher demand on airport pavements. Therefore, a study to adapt new design criterion is being performed to provide better built taxiways and runways for the growing fleet of large aircraft. In order to create new design criterion, the damage that the aircraft inflicts upon the pavement is closely studied. One of the most effective ways to study and account for the detrimental impacts is through full scale testing. Full-scale testing was and still is performed by the Federal Aviation Administration (FAA) at the National Airport Pavement Test Facility, NAPTF, (“About the NAPTF”, 2009) and also by the Airbus Industrie (Stac.aviation.civile.gouv.fr, 2009). The NAPTF builds full size pavement strips constructed with various cross-sections and strict quality control. The pavements built by the NAPTF are trafficked repeatedly by a vehicle with the ability to simulate the heavy aircraft with differing landing gear configurations and wheel loads. The FAA employs the testing of larger aircraft landing gear in a controlled environment to study the effects of wander and loading on airport pavement performance. The specific aspects impacting pavement design are discussed later in this chapter.



**Figure 2-0-a.** Airbus A380 Landing Gear Configuration



**Figure 2-0-b.** Boeing B777 Landing Gear Configuration

(AviationSpectator.com; SeattlePI.com, 2009)

### **2.2.1 National Airport Pavement Test Facility (NAPTF) Setup**

The National Airport Pavement Test Facility (NAPTF) located at the FAA William J. Hughes Technical Center, Atlantic City International Airport, New Jersey, USA opened for testing on April 12, 1999. The NAPTF is a joint venture between the Federal Aviation Administration (FAA) and the Boeing Company. The test facility consists of an indoor simulated runway 900 ft (274 m) long by 60 ft (18.3 m) wide. The test strips are constructed using techniques typical for runway construction. During construction, instrumentation is installed within the test strip to monitor responses of the pavement layers during trafficking. The test vehicle, shown in Figure 2-0-c, simulates a wide array of landing gear configurations with 1 to 10 wheels. Additionally, each load module, consisting of two wheels, on the landing gear has its own hydraulic cylinder allowing the wheel loading to be adjusted independently up to 75,000 pounds. This gives the test vehicle the ability to simulate aircraft with a weight approaching 1.3 million pounds. The test vehicle also simulates aircraft wander by varying the distance of the gears from the centerline of the test strip (National Airport Pavement Test Facility “About the NAPTF”). Wander is discussed in greater detail in a later section.

The NAPTF simulates testing in cycles known as “construction cycles”. Each construction cycle has its own unique characteristics, such as pavement type, subbase type, subbase depth, base layer thickness, and subgrade type. The duration of a construction cycle lasts many years from the construction phase to the analysis of the resultant data. The focus of this study is on construction cycles that have flexible



pavements. This study includes data from construction cycle 3 (CC3) and construction cycle 5 (CC5), which is the most recent construction cycle of interest. Figure 2-0-e shows a closer view of the landing gear configuration used at the NAPTF during Construction Cycle 3 (CC3). The rutting can be clearly seen in the pavement section of Figure 2-0-d. After the pavement sections are loaded to failure, post traffic testing and pavement removal is performed to prepare for the next construction cycle. The main purpose of this indoor test facility is to accelerate life cycle testing of a simulated airport pavement in a more controlled and cost effective environment; as opposed to building a full size outdoor runway to test empirical methods and runway design modifications (Garg 2007).



**Figure 2-0-c.** Enclosed Runway Test Strip with Test Vehicle  
(FAA.gov, 2009)



**Figure 2-0-d.** Northside of CC3 at  
19,500 Passes



**Figure 2-0-e.** Customizable truck in a  
six-wheel configuration

(FAA.gov, 2009)

#### **2.2.1.1 Data Collection (MDD) and Access (Database)**

Embedded in the pavement and support layers are instruments for dynamic data acquisition that collect data at a rate of 20 samples per second. Environmental instrumentation collects data about the surrounding environment at a rate of 4 samples per hour. Multi-Depth Deflectometers (MDD), shown in Figure 2-0-f and Figure 2-0-g are embedded in the test strips immediately after construction. The MDDs are a series of deflection sensors stacked vertically within a flexible tube. The assembly is inserted into a hole bored from the surface through all the layers and anchored to the bottom most layer. During trafficking, a series of MDDs record deflection data within the supporting layers for various sections of the simulated runway. The data are used to calculate deflections of the material layers during trafficking.



**Figure 2-0-f. Multi-Depth Deflectometers (MDD) Before Installation**



**Figure 2-0-g. MDD Installed in Test Strip**

(FAA.gov, 2009)

The recorded data are published by the FAA to their database

(<http://www.airporttech.tc.faa.gov/naptf/>), which is searchable using Structured Query Language (SQL) (SQL Server, 2005). The SQL database allows users to query for any available data provided that they had been given the proper access rights. The data is then returned in a tabular format that is easily manipulated into a spreadsheet program for further analysis by the user. The database returns values for MDDs, pressure readings, joint opening measurements, and strain measurements in both flexible and rigid pavements (Dong 2002).

Analysis of the data and material provides insight on the effects of wander and repeated loading under moving heavy loads on rutting and damage to the airport pavement. The testing performed at the NAPTF takes into account the simulation of wander, which is the offset of the vehicle's path of travel from the centerline of the test strip (Timm, 2005).

The wander pattern that is used for the majority of the traffic testing consists of 66

vehicle passes, arranged in 9 wander positions, known as tracks. The wander positions and sequences were chosen to simulate a normal distribution of aircraft traffic with a standard deviation of 30.5 inches (77.5-cm), representing the current design condition for airport taxiways. Normally, the same wander is used on both carriages (FAA.gov, 2009). Figure 2-0-h shows the normal distribution of the wander path of the test vehicle. More details on the effects of wander are discussed in subsequent sections.

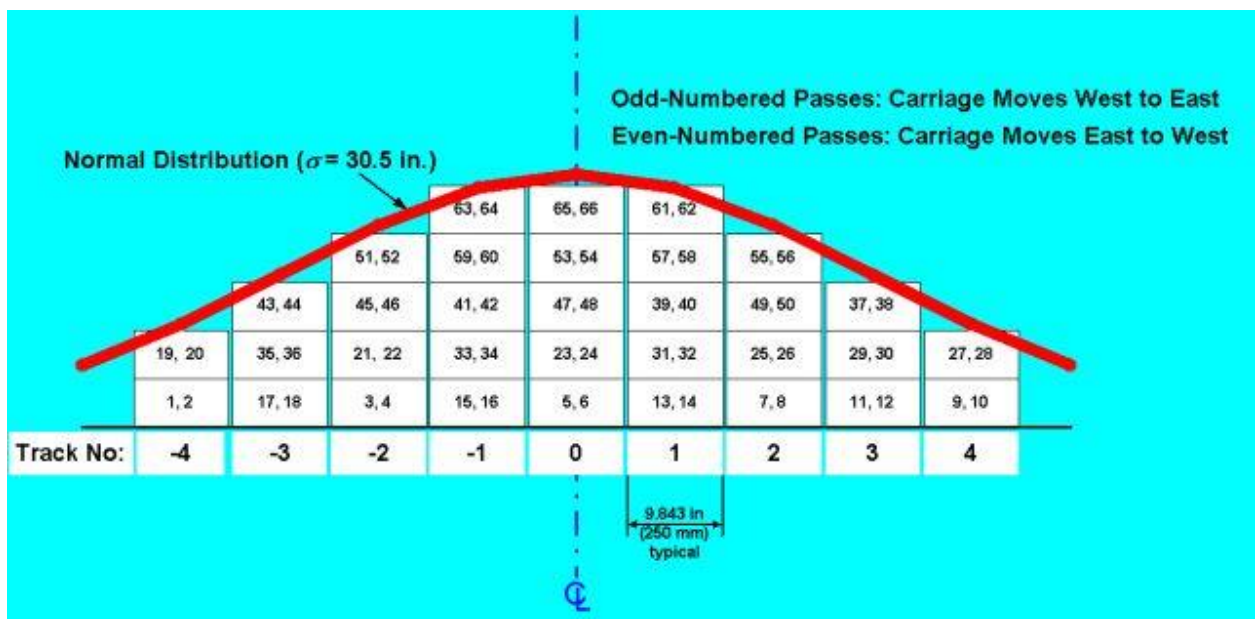


**Figure 2-0-h.** Normal Distribution Curve of Wander  
(FAA.gov, 2009)

### 2.2.1.2 NAPTF Findings

Construction Cycle 3 (CC3) includes flexible pavement sections, which are constructed using P-154 subbase and P-209 base courses, which are specified in the FAA's Advisory Circular No. 150/5370-10F Parts 2 and 3, respectively. The test pavement of CC3 consists of 4 flexible pavement test items, namely LFC1, LFC2, LFC3 and LFC4,

constructed over a low strength subgrade known as DuPont Clay. The test items are sections along the length of the construction cycle's pavement with further subdivided characteristics. Cross-sectional views showing pavement structures for each of the test items are indicated in **Error! Reference source not found..** Each test section is constructed with a different subbase layer depth. An increase in subbase thickness creates a stronger pavement structure.

LFC-1	LFC-2	LFC-3	LFC-4
127-mm P-401 SURFACE	127-mm P-401 SURFACE	127-mm P-401 SURFACE	127-mm P-401 SURFACE
203-mm P-209 BASE COURSE	203-mm P-209 BASE COURSE	203-mm P-209 BASE COURSE	203-mm P-209 BASE COURSE
406-mm P-154 SUBBASE COURSE	610-mm P-154 SUBBASE COURSE	864-mm P-154 SUBBASE COURSE	1092-mm P-154 SUBBASE COURSE
LOW-STRENGTH SUBGRADE CBR-3	LOW-STRENGTH SUBGRADE CBR-3	LOW-STRENGTH SUBGRADE CBR-3	LOW-STRENGTH SUBGRADE CBR-3

**Figure 2-0-i.** Cross-sectional Test Section Compositions of CC3

(FAA.gov, 2009)

CC3 has a significant amount of rutting in the P-154 crushed stone subbase layer, as illustrated in Figure 2-0-j.

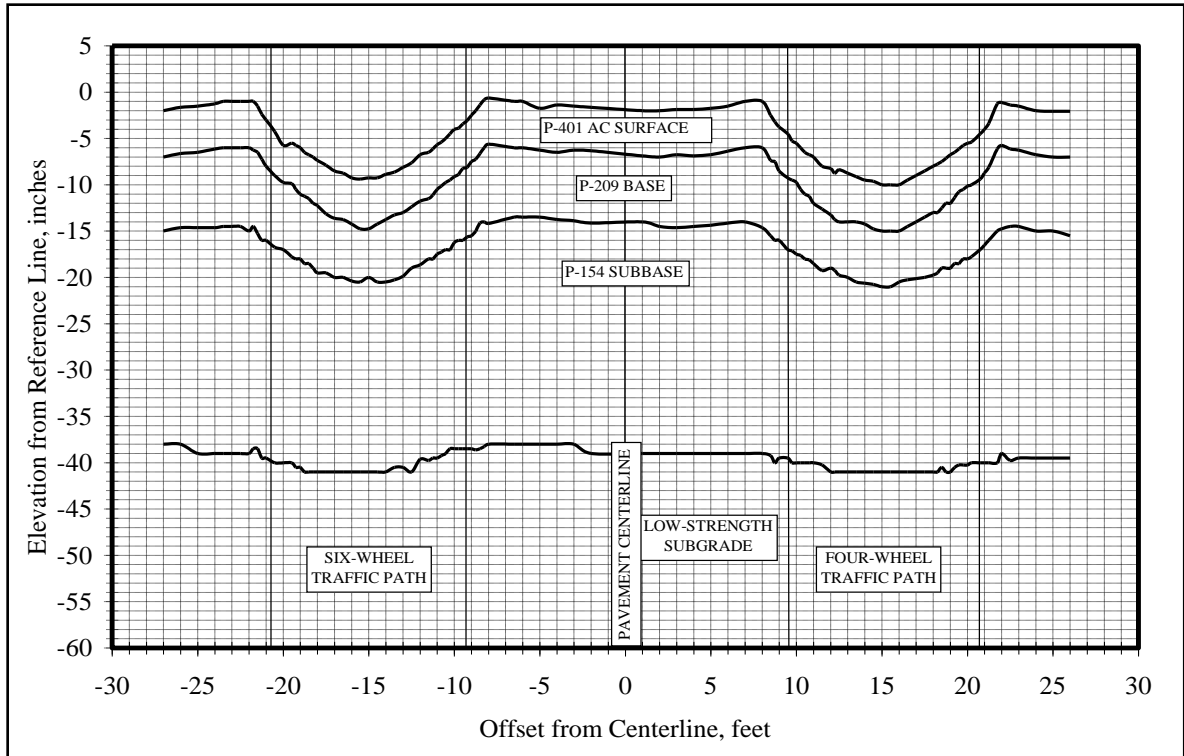


**Figure 2-0-j.** Cross-Section of Trafficked LFC-2 Test Item

Figure 2-0-j is a cross-sectional view showing the permanent deformation of the surface and layer interfaces in relation to the center of the test strip. Through the comparison of multiple test strips, it is shown that the behavior of the P-154 subbase is affected by the overall stiffness and thickness of the pavement structure (Garg and Hayhoe 2007).

Test item LFC1, the weakest structure of the four test items due to its shallow subbase, exhibits very large vertical pavement deformations from the beginning of trafficking as a result of shear failure in the subgrade. This appears well before a significant amount of compaction or shear failure of the subbase can take place. The subgrade shear failure leads to a “W” shaped transverse rut profile at the surface of the pavement that is characteristic of failure at low pass levels. In test item LFC2, major levels of compaction

in the subbase layer can be seen at medium traffic levels and continue even after the pavement fails structurally. In the thicker test items, LFC3 and LFC4, a large amount of compaction is observed in the P-154 subbase layer but less than that of LFC2. However, these test items require a larger number of passes at heavier wheel loads to reach failure. However, contrary to expectations, there is no significant increase in subbase densification (Garg 2007).

The findings of CC3 suggest that as the subbase layer thickness increases, the structure, as a whole, is more resistant to vertical loading and rolling action of the wheels. For instance, LFC2 suffers from severe rutting and significant densification of the subbase layer. However, in comparison with LFC1, which has a thinner subbase layer, the densification and failure takes a greater number of traffic cycles (LFC1). LFC3 and LFC4 show a considerable amount of rutting in the P-154 subbase layer. However, they lack a substantial amount of densification in the subbase layer despite the higher loads applied on these test items. This suggests that there may be a reshuffling or reorganizing of the particles causing reorganization of the subbase layer, but with little to no densification (Hayhoe 2006).

The findings from CC3 have a profound impact on the design and performance of CC5. CC5 is being utilized to study the effects of multiple gear configurations, subbase material depth, and material quality on the performance of flexible pavements. As with CC3, the test pavement of CC5 consists of 4 flexible pavement test items designated LFC1, LFC2, LFC3 and LFC4. Test items LFC-1 and LFC-4 are comprised of a subbase layer 34 inches thick. LFC-2 and LFC-3 both have a 38-inch deep subbase layer. The

granular subbase material commonly consists of one of two different materials including crushed quarry screenings, P-154, and dense graded aggregate (DGA). Additionally, 8 inches of P-209 crushed stone base material is placed above the subbase layer and lastly a 5-inch thick layer asphaltic concrete is applied to the surface (“Construction Cycle 5” 2011). A cross-sectional view of CC5 is illustrated in Figure 2-0-k.

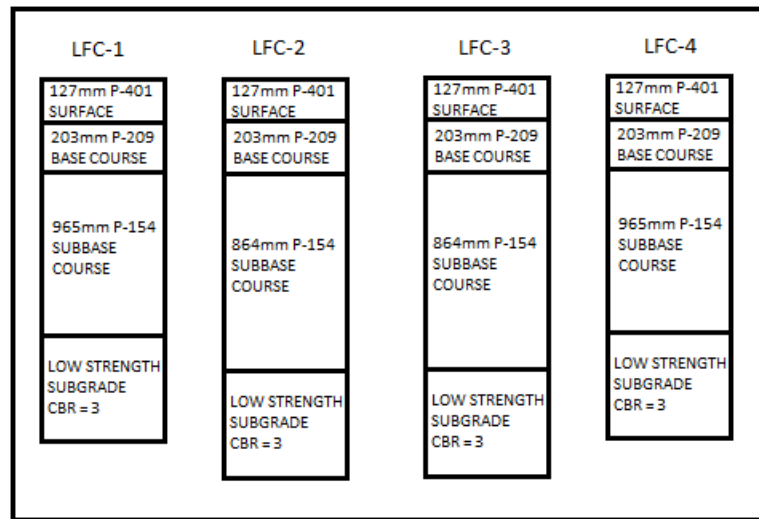


**Figure 2-0-k.** Cross-sectional Test Section Compositions of CC5

## 2.2.2 Airbus Testing

The A380 Pavement Experimental Program is being developed by the Airbus Industrie, the Service Technique des Bases Aériennes (STBA), and the Laboratoire Central des Ponts et Chaussées (LCPC). The main reason for introducing this program is to provide full-scale testing data to compare with the multi-layered elastic model predictions by the STBA and LCPC. The size and weight of the Airbus A380 necessitates the full-scale testing and elastic modeling to ensure the design of appropriate pavement structures. In addition, the study also aids in a greater understanding of the effects of different gear/wheel spacing and various Airbus aircraft landing gear configurations (Airbus



2001). Airbus's facility, located in Toulouse, utilizes materials representative of the four internationally recognized subgrade categories A, B, C and D for flexible pavement structures. The subbase thickness is varied based on the subgrade category and for comparison purposes. Airbus outfits each layer of the pavement structure with sensors to measure deflections (Airbus 2001).

The simulation vehicle simulates full-scale main landing gear configurations of various wide body aircrafts such as the A380, A340, B747, B777, and MD11. As many as 22 wheels are individually loaded to a maximum of 32 tons. The vehicle features variable dimensions for bogie position, wheels, and axle spacing.

#### **2.2.2.1 Airbus Testing and Differences from NAPTF**

Airbus testing is similar to the type of testing being conducted at the NAPTF. One of the major differences is that it is performed outside on a specially built runway. This differs from the NAPTF testing where a full scale indoor runway is used to avoid environmental variables.

#### **2.2.2.2 Airbus Study Findings**

The Airbus study is not looking specifically at the compaction or rutting effects due to trafficking, and as a result, does not expressly report their findings on the post-construction densification. The data available make it possible to carry out a realistic calibration of the linear elastic multi-layer model for the structures B, C and D, three of the four structures. This includes adjustment of the modulus of rigidity of the materials

and the subgrade, and the division of the thick layers of untreated materials to reproduce their nonlinear behavior. After the calibration, the elastic model of the multilayered structures is able to precisely define the maximum deflections at the top of the subgrade and subbase layers for structures B, C, and D (Airbus 2001).

The intention for all the full-scale testing is to collect data pertaining to the interactions of aircraft landing gear configurations and the effects of the increased loading due to the heavy aircraft on the life of the pavement and its supporting layers. By analyzing the data and comparing it to the analytical results obtained from software packages like ALIZÉ and FAARFIELD, the software packages are able to be properly calibrated and modified.

The improvements to the models create more accurate software packages that use more complex material models. As a consequence, future runway and taxiway designs will be able to better accommodate the new complex multi-wheeled and multi-gear configurations. By understanding these interactions and effects, the service life of future runways and taxiways can be more accurately predicted.

### **2.3 Multi-wheel Multi-gear Configurations**

It is very difficult to quantify the effects of multi-wheel multi-gear interactions. These effects vary by pavement thickness, load, tire size, temperature, and other factors.

Accurate modeling of these effects is nearly impossible due to the complexities introduced by the different multi-wheel multi-gear interactions. For this reason, some

generalizations are made and some of the minor factors are neglected to help develop more practical computer models.

Permanent load-induced deformations are developed at points within a flexible pavement structure and subgrade. The aggregate effects of the deformations produce permanent surface deformations. Design methods used in practice do not attempt to model this deformation process; deformations of individual soil elements are not computed and totaled to give predictions of surface deformations (Rodway 1999). For this reason some modeling studies obtain plots showing vertical strain rather than vertical deflections because vertical deflections seem to over predict rutting as wheel loading increases. It is important in the creation of new design standards that data relevant to newer plane landing gear configurations be used as these configurations are more complex and heavier than ever before.

## **2.4 Effects of Wander**

One of the key problems facing airport runways and taxiways is the effect of wander. Many studies and simulations exist that have attempted to determine the influence of wander on pavement performance. Donovan (Donovan 2007) examines the data from NAPTF and finds that wander can negate the stiffening in unbound granular layers and create a pavement more susceptible to increased deformations. Wander induces the anti-shakedown effect which is a potential cause for more deformation than if aircraft wheels were to travel in a straight pass time after time. Shakedown is the theory that an elastic-plastic structure will shakedown to a purely elastic state after a specific amount of plastic

deformation. Anti-shakedown effect is caused by rearrangement of the particles within the pavement system that takes place due to the constant change in the path of the loading. The movement negates any shakedown expected in the unbound aggregate (Donovan 2007).

This problem can be mitigated with a better understanding of the effects of repeated loading (such as loading caused by a rolling aircraft landing gear) over a long period of time, such as the lifetime of an airport taxiway or runway. There remains the possibility that the effect of post-construction densification is one of the leading contributing factors to the reduction of stability of a runway structure. If one section of a runway is weakened due to repeated heavy trafficking, the effect of trafficking over the edge of that section could cause a reduction in the strength of the adjacent section due to “shuffling” of the particles making up the layers supporting the pavement surface. As a result, the region of weakness propagates throughout the width of the runway reducing the strength of the entire structure.

This anti-shakedown effect or rearrangement of particles is mainly due to post-construction modification or densification (compaction) of the base and/or subbase layers. In order to fully appreciate the anti-shakedown effect, construction compaction and subsequent post-construction densification due to trafficking and wander must be fully comprehended. After a better understanding of compaction and interaction of the particles in the base and subbase layer during construction and trafficking is obtained, it may be possible to better predict the life of a pavement and mechanism of failure. The

ultimate goal is to use this knowledge base to modify construction techniques and machinery to allow for better compaction during the construction process, leading to a longer and more stable service life for the runway. Examples of construction techniques and machinery are explained further in the following section.

## **2.5 Compaction**

### **2.5.1 Field Construction Compaction (Construction) Methods**

There are four common methods used for field compaction at present. These are the Smooth-wheel rollers, Pneumatic rubber-tired rollers, Sheepsfoot rollers, and Vibratory rollers, shown in Figure 2-0-1. Smooth-wheel rollers are not suitable for producing high unit weights when used on thick layers, but are suitable for proof rolling subgrades and for finishing operations of fills with sandy and clayey soils. Pneumatic rubber-tired rollers are comprised of a series of tires (typically four to six wide) mounted in parallel at close spacing. The assembly is then heavily loaded and rolled to compact sandy and clayey soils. These rollers typically exert twice the contact pressure as smooth-wheel rollers and use a combination of pressure and kneading action to compact the soil. A sheepsfoot roller is a drum roller that has a large number of projections, which make the roller capable of two to ten times the contact pressure of the pneumatic rubber-tired rollers. The sheepsfoot roller is the most effective in compacting clayey soils (Das 2010). This is a result of the intense kneading action exerted by the roller on the soil. The addition of a vibratory mechanism to any of the smooth-wheel rollers, pneumatic rubber-tired rollers, or sheepsfoot rollers increases the effectiveness of the compactor in granular soils. The vibrations induce self-kneading in a granular soil by promoting the

rearrangement and shifting of the particles. In most cases, the compaction of materials in the field are specified as a percent of maximum dry density obtained from Standard Proctor or Modified Proctor tests, ASTM D698 and ASTM D1557 respectively.



**Figure 2-0-1.** Common Roller Types: Smooth-wheeled roller (top left), pneumatic rubber-tired roller (top right), Sheepsfoot roller (bottom left), and the internal vibratory attachment (bottom right).  
(Cat.com, 2012)

## **2.5.2 Laboratory Compaction**

### **2.5.2.1 Standard and Modified Proctor Tests**

The Standard Proctor test, developed in 1933, is one standard test for specifying the compaction properties for soils. The test requires a cylindrical mold with a volume of  $1/30 \text{ ft}^3$  and a 4 inch diameter. The sample is compacted in the mold at user specified moisture contents in three equal layers by dropping a 5.5 lb hammer 25 times per layer.

The drop height of the hammer is 12 inches for each blow. By performing this test at a range of moisture contents, the optimum moisture content is determined. The optimum moisture content is defined as the moisture level at which the soil is capable of reaching its maximum theoretical density. Additionally, the Proctor test allows for a larger mold with a diameter of 6 inches to be used, but 56 blows per layer are necessary with this larger mold to ensure that the same energy is input per unit volume of soil. The larger mold is crucial for testing soils containing large aggregate. Compaction during construction in the field is often specified as a percentage of Standard Proctor density, ASTM D698. Standard Proctor density is the maximum dry density of the soil at its optimum moisture content as determined by the Standard Proctor test.

Presently, compaction machinery is much heavier and more efficient than equipment in use during the development of the Standard Proctor test. This significantly increases the construction capabilities by producing higher dry densities in the field. This renders the standard proctor test obsolete in many cases and gives way to the modified proctor test. The procedure is similar to the Standard Proctor test. However, the Modified Proctor test requires a 10 lb hammer dropped from a height of 18 inches in 5 layers,. Informative diagrams of standard and modified Proctor tests are shown in Figure 2-0-m. A graphical representation of the tests' moisture content plotted against dry density is known as the Proctor curve. A typical Proctor curve can be seen in Figure 2-0-n along with the optimum moisture content and maximum dry density.

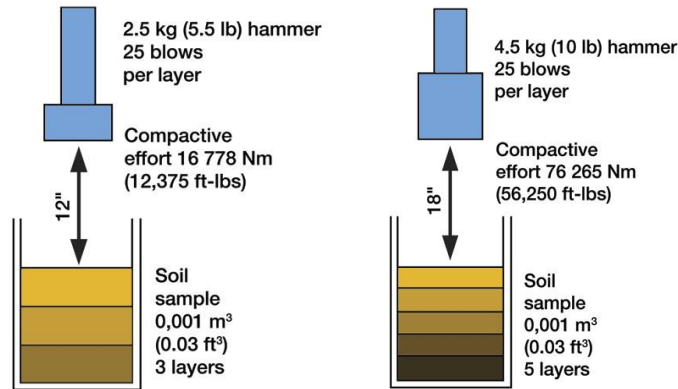


**Figure 2-0-m.** Visual Description of the Proctor Tests and a Typical Proctor Curve (Das, 2010)

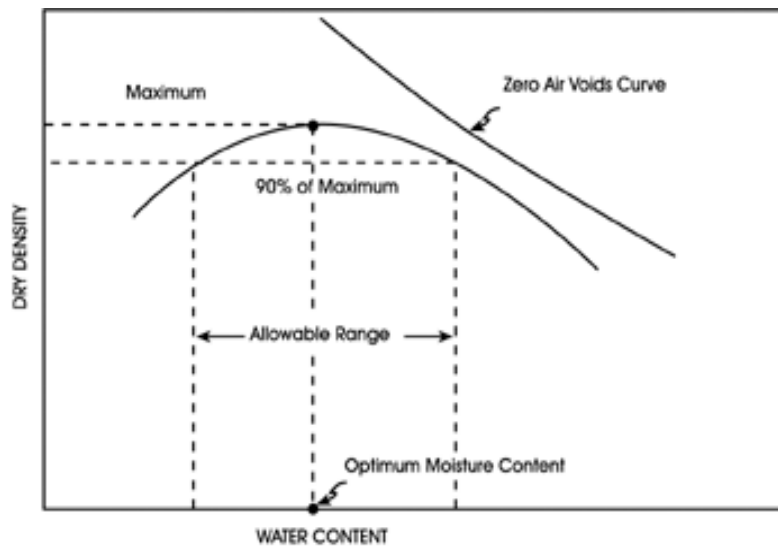


**Figure 2-0-n.** Diagram of Proctor Curve

The density of any soil in a given state is expressed as a percent relative to the theoretical maximum density of that particular soil according to the Standard or Modified Proctor test, which is known as relative compaction (Das 2010). The major disadvantage of the Proctor test is dropping a hammer vertically means the energy for compaction comes solely from the vertical impact of the hammer. This differs from the mechanism of compaction employed by the field equipment described in 2.5.1. The construction



equipment relies on a combination of vertical loading from the machine weight and kneading/shearing action that the roller and vibratory attachment produce, if so equipped. This is one major advantage of the Superpave Gyratory Compactor (SGC) described in 2.5.2.2. The SGC is run extensively for asphalt performance testing, but also shows promise for use in the performance testing of unbound materials.

#### **2.5.2.2 Superpave Gyratory Compactor (SGC)**

The Superpave Gyratory Compactor (SGC), shown in Figure 2-0-o. Troxler Superpave Gyratory Compactor and Illustration of Sample Mold OffsetFigure 2-0-o, is a crucial tool for the compaction and analysis of hot mix asphalt (HMA) samples. Standards and procedures for testing of HMA mixtures from societies such as the American Society for Testing and Materials, ASTM, and the American Association of State Highway and Transportation Officials, AASHTO are well established (AASHTO T312-04, 2004) (ASTM D6925/D7115/D7229). Only recently has there been a growing interest in the possibility of using the SGC to compact soil samples. Many recent studies on unbound materials base their testing procedures on the standard procedures for testing HMA. There are several different reasons for the interest in the possibility of using the SGC for compaction and life cycle testing of soil and unbound material. This is summarized in Section 2.6.

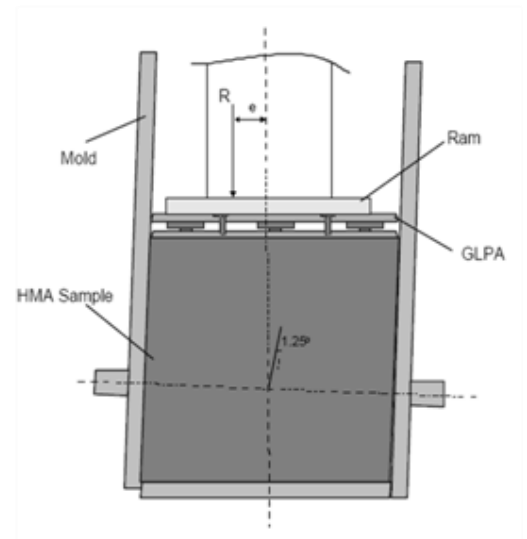


**Figure 2-0-o.** Troxler Superpave Gyratory Compactor and Illustration of Sample Mold Offset  
(DOT.gov, 2009)

### 2.5.3 Compaction Mechanics

#### 2.5.3.1 Interlock

There are several different factors that affect the shear strength properties of a soil.

Factors that influence the stress-strain behavior of soils are classified as inherent, intermediate and external factors. Inherent factors are properties that are material

dependent and include particle size, particle size distribution, shape, angularity, and

surface roughness. Other inherent factors that influence stress-strain behavior are

hardness of the particles, mainly influenced by the mineral content, and specific gravity

distribution. The problem is that particle shape is difficult to measure and classify.

Angular, sub-angular, sub-rounded and rounded are the general terms used to describe the general shape of the particles (Das 2010). Angular particles have sharp edges and

corners, while rounded particles tend to have smoothed edges and very dull (if any)

corners. For example, a broken piece of glass with sharp edges and corners is an angular

shape while a ball with very smooth edges and not very easily distinguishable corners is considered rounded. The general shape is one reason that the soils with angular particles were harder to compact effectively due to particle interlock. Interlock resists relative displacement, but causes breakage and crushing under loading. Rounded particles do not interlock and usually resist crushing and breakage (Swan, 2009).

Particle interlock dictates compaction characteristics as well as shear strength after compaction. Typically, more interlock between particles increases the strength of the compacted material as a whole. One of the biggest contributing factors to the interlock strength is the moisture content. Typically, as the moisture content increases, the interlock of the material is reduced slightly. Essentially this means that a moist soil is more easily compacted than the same soil in the dry state. This is discussed in more detail in section 2.5.3.2.

#### **2.5.3.2 Moisture Content**

Compaction is generally defined as the densification of soil by the removal of air, which requires mechanical energy. The addition of water during compaction acts as a lubricating agent allowing the particles to be rearranged more efficiently. Therefore, by introducing water it is easier for the aggregate to move into a denser state (Das 2010). As the moisture in a soil increases, the maximum dry density of the soil reached through compaction also increases. However, studies show there is a point at which this increase in maximum dry density begins to diminish. Once the soil reaches a specific moisture content, which is unique to the material, the additional moisture impedes the densification

of the material. Findings show that this is due to the water occupying the space that could have been otherwise occupied by the soil particles. The moisture content at which the highest maximum dry density is obtained is referred to as the Optimum Moisture Content (OMC). OMC is typically found by use of either the Standard or Modified Proctor test, as described above (Das 2010). A typical Proctor curve is seen in Figure 2-0-nFigure 2-0-n. Diagram of Proctor Curve. The highest point along the curve defines the OMC and maximum Dry Density of a soil.

The maximum dry density at the OMC is typically used as the standard to which field compaction values are compared for a certain soil. Densities of soils compacted in the field are typically referred to as a percent relative to the Proctor density, or relative compaction. A slight change in the moisture content of a soil is one of the simplest ways to affect the dry unit weight of the soil after compaction. Exploring the practicality of using the SGC to accomplish this is being thoroughly investigated. Some studies use the SGC to compact soil but the primary use of the machine still remains as a means of testing compaction and degradation of hot mix asphalt (HMA). Therefore, testing of soils by use of an SGC is a relatively new idea (Mokwa 2008).

### **2.5.3.3 Crushing**

Compaction and strength of the material after construction is influenced by the interlock of the particles as discussed in 2.5.3.1. However, the interlocking itself is sometimes affected by crushing of the particles during construction compaction and subsequent trafficking. Crushing is a general term that encompasses fracture, attrition, and abrasion

of particles in a soil. Fracture occurs when a particle splits into two or more particles of similar size. Attrition occurs when the particle remains intact with the exception of the breakage of sharp points or edges. Finally abrasion is said to occur when any part of the particle is removed, resulting in the production of fines. These three modes of crushing are illustrated graphically in Figure 2-0-p (Ramamurthy 1974).

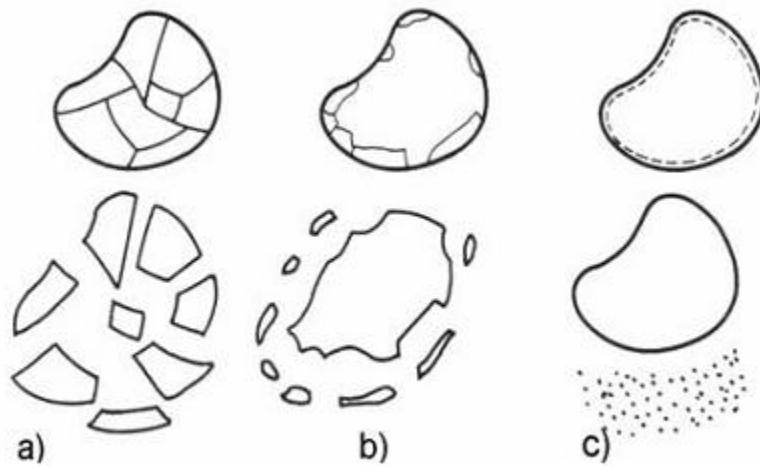


**Figure 2-0-p.** Illustration of Aggregate Breakage Modes (a. fracture, b. attrition, and c. abrasion)  
(Ramamurthy, 1974)

It is important to consider the possibility of crushing when discussing the strength of a material in its compacted state. When a compactor moves over the material, or a vehicle rolls over the constructed surface, the particles of the material experience shear forces as they shift. The shift of the material is considered a primary cause of all breakage. All of the methods of breakage described above change the grain size distribution of the material as well as the angularity and shape of the aggregate. This has an enormous impact on particle interlock. For example, when attrition occurs, any sharp points or edges are broken off the particles. This results in a reduction of interlock, which can

cause a decreased ability to support weight during loading. If a great deal of abrasion takes place, the particle angularity is reduced and produces a more spherical aggregate. This also reduces the aggregate to aggregate interlock within the soil, ultimately reducing the strength of the material. This breakage could be a result of construction compaction or repeated loading, such as a taxiing aircraft. For this reason there is a great deal of concern as aircrafts become heavier and more complex. There is concern due to the increase in potential for breakage of the materials constituting airport pavement surfaces.

Breakage of the material is generally considered a negative aspect of the construction process. This is one of the major reasons for varying the moisture content of a soil as described in 2.5.3.2. Increasing the moisture content of soil lubricates the particles and allows them to more easily rearrange into a denser state, while minimizing the amount of breakage. The problem stands that the accepted testing methods such as the Standard and Modified Proctor tests use vertical impact loading and cause fracturing of the particles; which does not closely simulate the actual forces, such as shear force, seen during construction. Simulation of shear forces and compressive loading exerted by moving machinery and vehicles is more closely simulated by the Superpave Gyratory Compactor.

## **2.6 Laboratory Testing Using the Superpave Gyratory Compactor**

The Superpave Gyratory Compactor (SGC) testing standard is used for the determination of volumetric and mechanical properties of asphalt mixtures. The Strategic Highway Research Program was a federal research initiative to evaluate techniques to prevent the deteriorating conditions of the nation's highway system and to improve performance,

durability, safety, and efficiency. The SHRP recommends this style of compactor because it produces specimens similar to pavements in both aggregate orientation and mechanical properties. Additionally, it is useful for quality control at hot-mix plants. Operation of the SGC requires preparing a sample in the mold, which is then inserted in the machine. The top of the mold is aligned with the center axis of the compaction ram. The bottom of the sample mold is then offset by a certain number of degrees from that vertical axis. The bottom is designed to be gyrated around the offset axis at a set rate. During the gyration process, the vertical ram applies pressure from the top. As the specimen is compacted, a pressure gauge signals the loading system to adjust the position of the loading ram so that the pressure remains constant throughout the compaction process. Compaction occurs due to the pressure from the ram and the kneading action provided by the revolving angle (“Bitumous Mixtures Laboratory” 2009).

### **2.6.1 SGC Readouts and Settings**

The Troxler Model 4140, shown in Figure 2-0-o, is one of many SGC’s that allows for user adjustment of all the variables that affect the densification and processing of a sample. The programmable variables include the angle of gyration, ram pressure, and rate of gyration. There are standards for testing asphalt that allow for the production of comparable samples for determining density and predicting life of the asphalt layer as well as determining field control parameters of hot mix asphalt production processes.

The AASHTO design standard T 312-04 specifies that the machine must be set to apply and maintain a pressure of  $600 \pm 18$  kPa perpendicular to the cylindrical axis of the specimen and that the compactor has to tilt the specimen molds at an internal angle of

$1.25 \pm 0.02^\circ$  and gyrate the specimen molds at a rate of  $30.0 \pm 0.5$  gyrations per minute throughout the compaction process (AASHTO T 312-04).

The SGC is equipped to record the height of the ram head at each gyration during the compaction process. The height data from the SGC can be transferred to a computer. The combination of the height of the sample at a given gyration with the known diameter of the mold determines the volume of the sample at a given time in the compaction process. By knowing the mass of the sample being used and the volume, the density of the sample can be determined at any point in the compaction process.

Sample compaction is run simultaneously with a device called the Pressure Distribution Analyzer (PDA), described in 2.6.2. The height data recorded by the SGC is correlated with the PDA data to gain insight on energy input by the SGC.

### **2.6.2 Pressure Distribution Analyzer for Energy Analysis**

The Pressure Distribution Analyzer (PDA) shown in Figure 2-0-q is a device that has a set of three load cells which measure and analyze all the forces acting on a sample during compaction. The PDA is useful for the calculation of the shear and vertical energy being applied on the sample during the testing process (TroxlerLabs.com 2009). A combination of the data collected by the SGC with that of the PDA creates a means of determining the total energy, vertical work, and shear work for each gyration.





**Figure 2-0-q.** Pressure Distribution Analyzer (PDA) and Schematic Representation, right (TroxlerLabs.com 2009)

### 2.6.2.1 Vertical Work

The vertical work done is due to the vertical confining pressure applied. This pressure causes much of the vertical compaction of the sample by pressing the particles together and allowing them to rearrange naturally. The equation for vertical work is shown below.

$$W_{vertical} = PA\Delta h \quad \text{Equation 1.}$$

Where

$W_{vertical}$  = Vertical Work,

$P$  = Vertical Load,

$\Delta h$  = Height Change,

$A$  = area of sample

### 2.6.2.2 Shear Work

The major difference that separates the Proctor tests from the SGC testing method is that the gyratory action of the SGC causes a shear action within the sample. This shear action

simulates the kneading action of rollers used to compact asphalt concrete pavements by applying a vertical load to an asphalt mixture while gyrating a mold tilted at a specified angle (“Bituminous Mixtures Laboratory” 2009). This remains the reason that the SGC is used to simulate the construction of asphalt surfaces. Since the SGC mechanism closely represents the stress path applied during construction and trafficking, there is some interest in the possibility of using the SGC to determine the behavior of unbound layers of roads and airport pavements. The equation for shear work is shown below.

$$W_V = \frac{4Pe\theta}{Ah} \quad \text{Equation 2.}$$

where

$W_v$  = Shear Work,

$e$  = eccentricity,

$A$  = area of sample, and

$h$  = thickness of sample

### 2.6.3 Previous Studies Using the SGC on Soil

Currently, there is a growing interest in the possibility of using an SGC device to predict the construction compaction and lifecycle of soils being used in base, subbase, and subgrade of roadways, runways, and taxiways. Several studies exist that investigate the use of the SGC for soils ranging from granular soils to clays. Many of these studies investigate by basing test procedures on approved asphalt testing procedures and varied the test parameters such as the angle of gyration, rate of gyration, number of gyrations, and other SGC test equipment variables to determine appropriate values.

One study at Florida State University (Ping 2002) explores the possibility of using the SGC to better predict the response of sandy soils to modern construction equipment. The testing done is compared to Modified Proctor testing performed on the same soil to verify that the results were at least similar to the accepted methods. The study shows that the rate of gyration has little effect on compaction of sandy soils. Therefore, the gyration rate was held at the standard 30 gyrations per minute used for asphalt testing. However, the gyration angle, pressure, and moisture content of the soils in the study vary. In summary, findings show that varying the vertical stress, as a way of increasing the dry unit weight had little to no effect when the vertical pressure is above 200 kPa. Ping uses a maximum confining pressure of 500 kPa during all testing. The angle of gyration is reported to have some effect on the dry density of the sample when the number of gyrations is low, but the effect is minimal when the number of gyrations is increased. By varying the moisture content and keeping all other variables constant from test to test, the study shows that a moisture content and dry density curve can be plotted that resemble a Modified Proctor moisture content curve. The most significant finding of this study is that the number of gyrations has the biggest impact on the dry density of the samples. More gyrations equates to higher dry densities (Ping 2002).

A separate phase of the study performed at Florida State University (Ping 2003) investigates the effect of increased energy input on the dry density of the sample. In this phase, the pressure, number of gyrations, angle of gyration and gyration rate vary. By keeping the moisture content similar throughout testing, the study focuses on varying the compactive energy input into the sample. A test performed on A-2-4 sand shows that

varying the gyration rate from 10 to 20 to 30 gyrations per minute has no effect on the final dry density when all other variables are held constant. Additionally, findings show that the number of gyrations has a significant impact on the final dry density of the sample as was concluded from the previous study; more gyrations result in higher densities. Additionally, at low gyration numbers the gyration angle has a significant impact on the densification but this impact diminishes as the gyration count increases. In the 2003 study, an increase in vertical pressure did not have a major influence on the final dry density (Ping 2003). The results are shown in Figure 2-0-r through Figure 2-0-u.

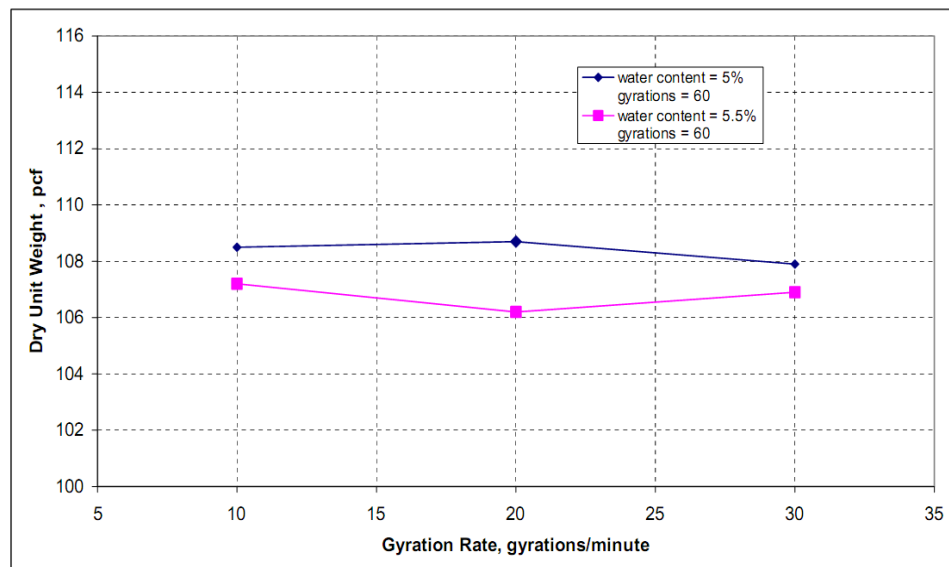


**Figure 2-0-r.** Compaction Curves for A-2-4 Soil with 12% fines at Various Gyration Rates (Ping 2003)

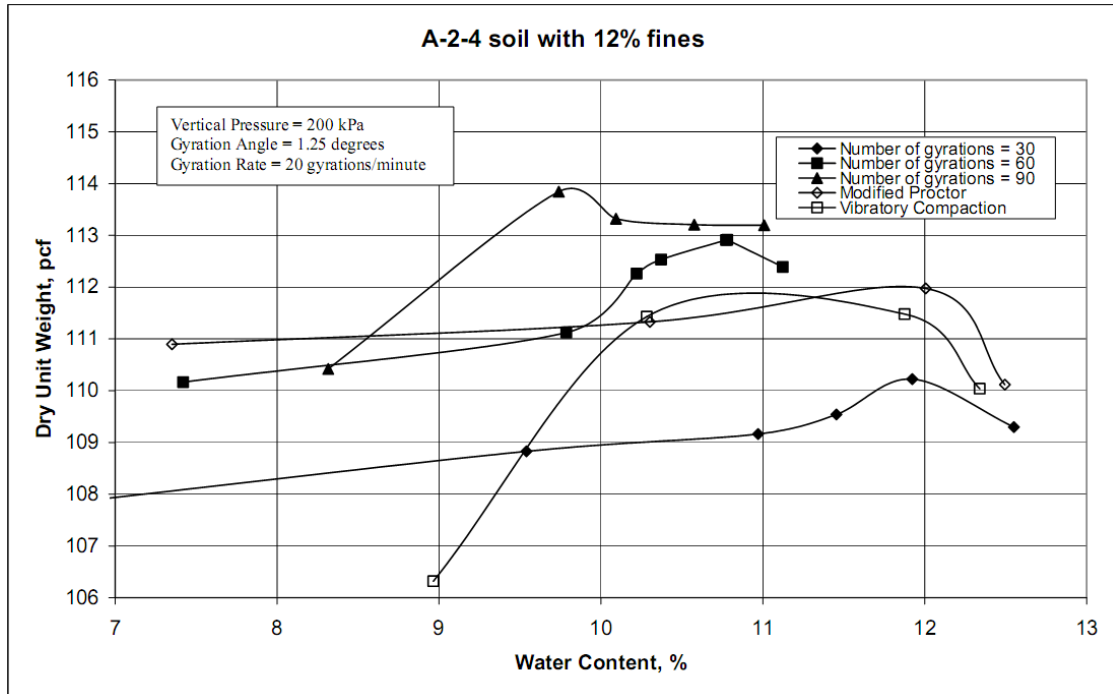


**Figure 2-0-s.** Compaction Curves for A-2-4 Soil at Various Gyration Counts

(Ping 2003)

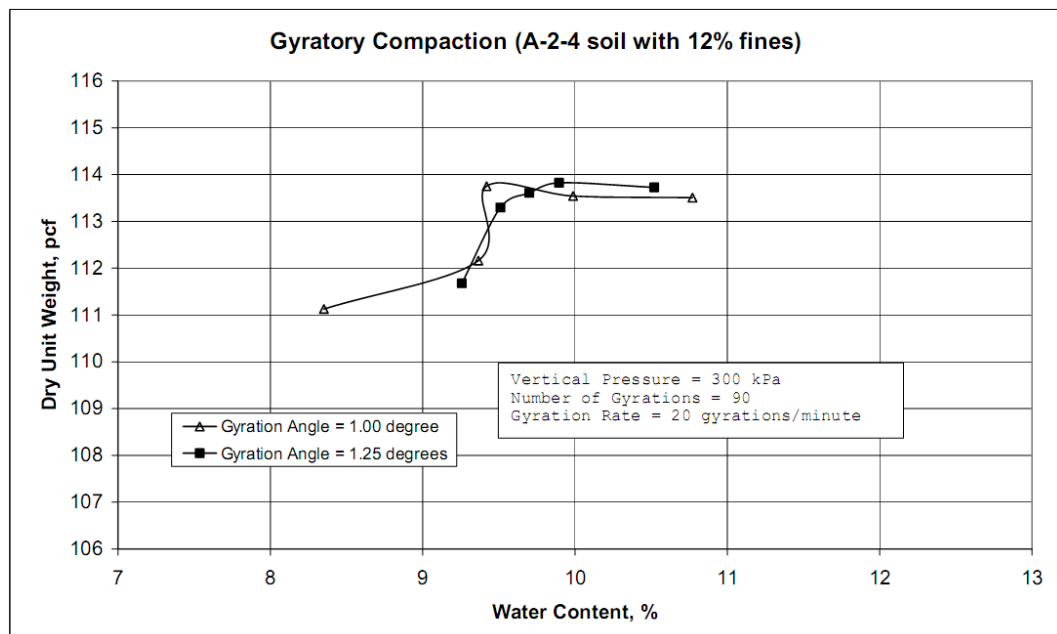


**Figure 2-0-t.** Compaction Curves for A-2-4 soil at Varied Gyration Angles (Ping 2003)

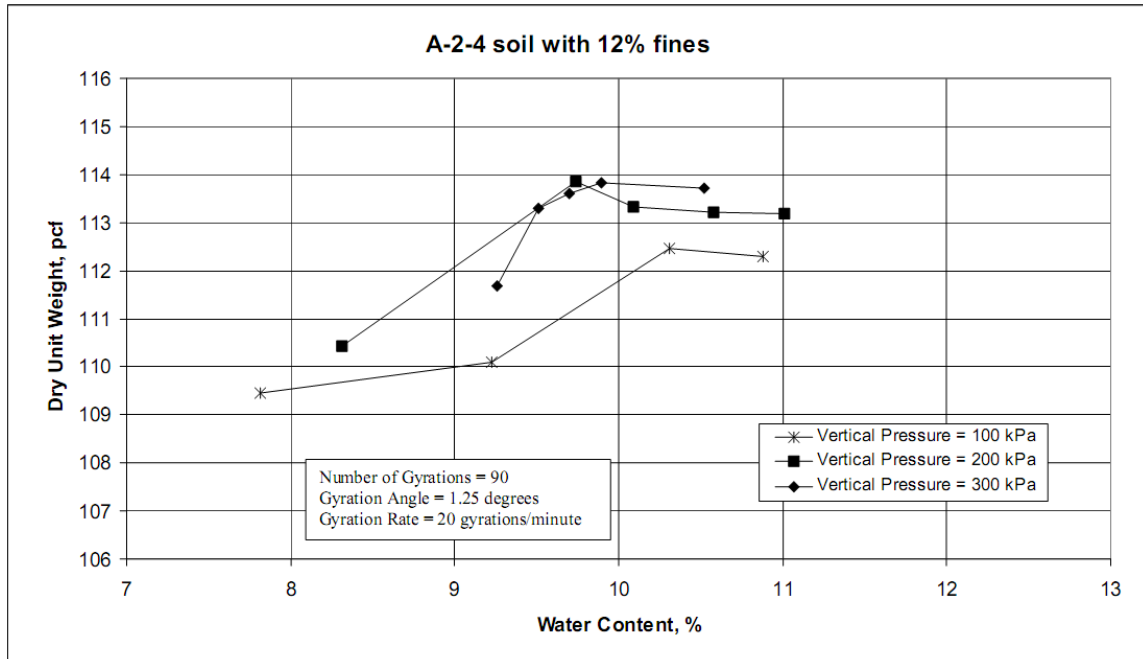


**Figure 2-0-u.** Compaction curves for A-2-4 soil at Various Pressures (Ping 2003)

Another study performed at Montana State University focuses on varying only the pressure and moisture content of the soils. Four different representative soil types are investigated with AASHTO Classifications of A-1-a (gravel), A-3 (sand), A-4 (silt), and A-7-6 (clay). The standard asphalt testing values are used for the gyration rate, angle of gyration, and number of gyrations. The pressure varies from 200 kPa to 600 kPa in 100 kPa increments and the moisture content vary from dry to saturated for each soil. This test shows that for the A-1-a gravel, the most effective means of increasing dry density is to increase the number of gyrations. The A-3 sand is influenced partly by the confining pressure but the most effective way to increase dry density of the sample is to increase the number of gyrations. The densification of the A-4 silt and the A-7-6 clay is affected the most by changes in the confining pressure. Comparison of the testing data shows that dry density and moisture content curves are very similar to Standard and Modified

Proctor tests as shown in Figure 2-0-v, even though the compaction mechanism used by the SGC is significantly different than that of either of the Proctor tests (Mokwa 2008).

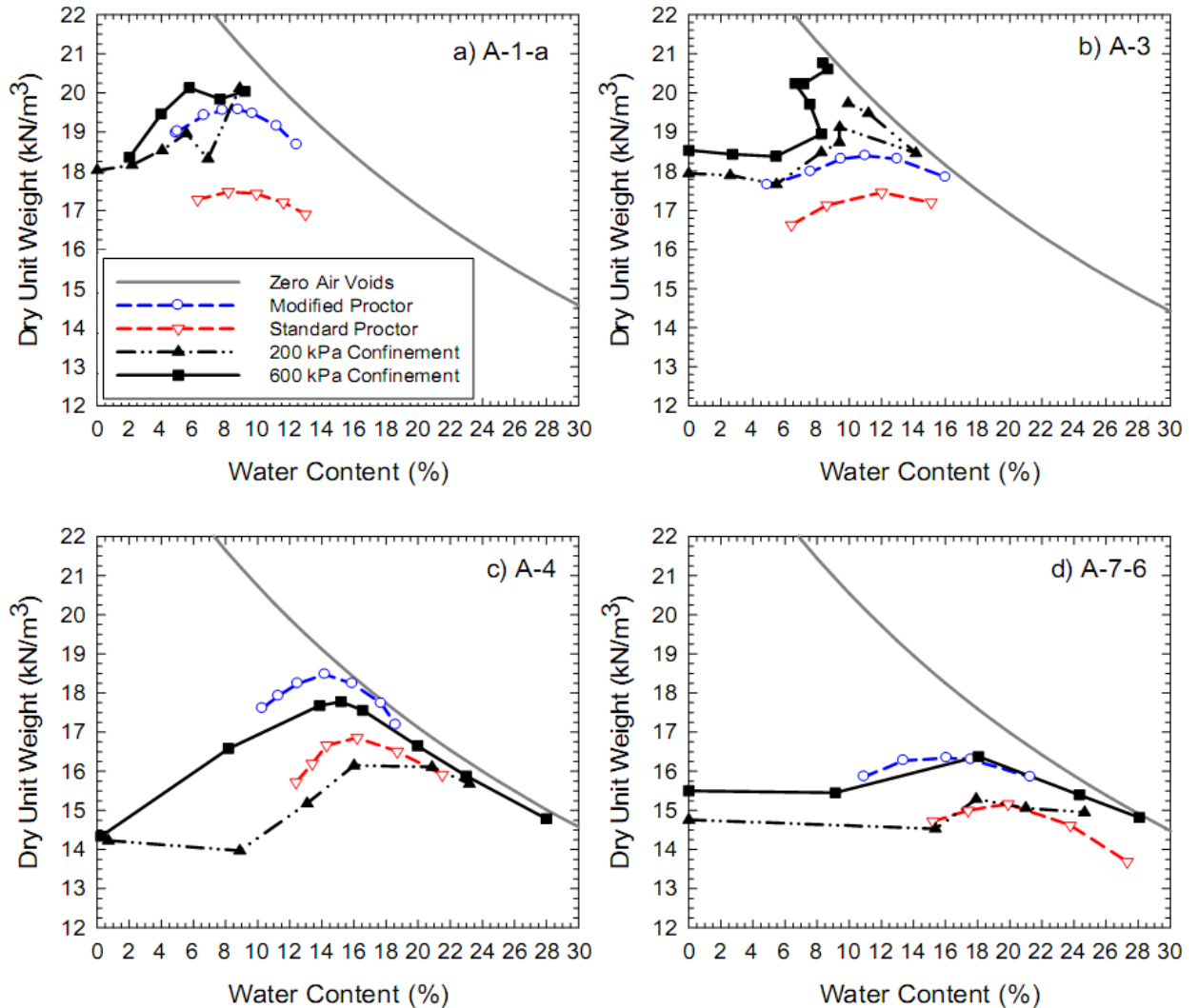


**Figure 2-0-v.** Comparison of Proctor Curves to Curves Compiled using SGC Data (Mokwa, 2008)

These studies demonstrate the possibility of using the SGC to simulate the compaction and lifecycle of unbound soils commonly used for roads and airport runways/taxiways.

Many of the studies start their testing based on the standards set for testing asphalt, due to the SGC's origin as a device for testing the compaction and life of asphalt mixes. Some

of the studies from earlier in this chapter imply that all granular soils, gravels and sands, tend to behave similarly in the SGC; cohesive soils, silts and clays also behave similarly in the SGC. However, the two classes, granular and cohesive, behave differently. Gravels and sands are not significantly affected by changes in the rate of gyration (up to 30 gyrations per minute) or by changes in angle of gyration when a substantial number of gyrations are performed. It is also shown that for the 200 kPa to 600 kPa range of confining pressure, an increase in the confining pressure is not an effective means of increasing final dry density. The variables that have the most significant impact on the final dry density are the moisture content and the number of gyrations. Testing of the cohesive soils shows that the confining pressure has the greatest influence on the final dry unit weight of the samples. For cohesive soils it is seen that an increase in the number of gyrations results in a relatively small increase in compaction. As a result of the knowledge gained from the literature review, a set of testing goals was compiled.

## **2.7 Testing Goals**

The idea of testing cohesionless and cohesive soils by use of an SGC is developing more interest as years pass. Standard testing procedures like the Standard Proctor and Modified Proctor testing methods have been available since the 1930's and are now becoming obsolete. The Proctor tests define what is often considered the maximum theoretical dry densities for soils to be achieved by construction. However, recent improvements in the size, technology, and capabilities of construction equipment have made it possible to reach greater densities in the field than these tests are capable of producing in the lab. For this reason there is much interest in the possibility of using the



Superpave Gyratory Compactor (SGC) to test soil samples in the lab to determine OMC and Maximum Dry Density, as well as the potential to simulate the life cycle of these soils in an accelerated manner. The SGC is being explored as a means to more closely simulate the actual compaction process used in the field during construction due to its gyratory action. A comprehensive analysis of compacted soil specimens in the SGC is needed for a better understanding of the mechanisms of compaction and how different variables affect the compaction process.

Full-scale testing like that performed at the NAPTF, provides valuable data on the effects of repeated loading and trafficking of airport taxiways. One potential use of the Superpave Gyratory Compactor (SGC) is to simulate the construction and trafficking compaction of the granular materials used to construct the full-scale test segments. The ultimate goal of this study is comprised of three parts:

- Examine the practicality of using the SGC to simulate compaction and define parameters to possibly replace or accompany the Standard and Modified Proctor tests in defining soil compaction characteristics.
- Gain a better understanding of the mechanisms that affected compaction and post-construction densification observed in the NAPTF full-scale tests.

- Investigate the possibility of using data from full-scale testing to correlate the post-construction densification behavior (observed during repeated trafficking, of the base and subbase materials) to SGC data.

## Chapter 3

### Laboratory Testing Results

#### 3.1 Material Classification and Properties

Materials were characterized in standard laboratory tests to verify particle morphology, size distribution, and compaction performance characteristics. These tests included the Modified Proctor test (ASTM D1557) and the Sieve Analysis (ASTM C136). The results of these tests can be seen in Table 3-0-a including the resulting soil classification performed using the AASHTO Soil Classification System (AASHTO M145).

**Table 3-0-a.** FAA P-154, DGA, and P-209 Material and Classification Properties

<b>Properties</b>	<b>P-154</b>	<b>DGA</b>	<b>P-209</b>
Maximum Modified Proctor (pcf)	135	154	156
Optimum Moisture content (%)	6.9	4.9	5.3
Coefficient of Curvature, Cc	3.3	3.2	2.0
Mean Particle Size, D50	1.5 mm	9.9 mm	6.4 mm
AASHTO	A-1-b	A-1-a	A-1-a

#### 3.2 P-154 Laboratory Experiment Results

In order to obtain a baseline for comparison of the SGC results, Modified Proctor tests at different moisture contents were performed according to ASTM D1557. The Modified Proctor test was completed using 25 blows per layer and a 934.46 cubic centimeter mold. The first set of SGC tests were conducted on the P-154 material. These tests were conducted with a gyration angle of 1.25 degrees at three different pressures, 600, 800, and 1000 kPa. A density at 85 percent of the Modified Proctor density was considered the baseline for loose compaction from the field compaction results. It was evident from

the test results that the compaction rate was affected considerably by both the confining pressure and the moisture content.

The sample sizes tested in the SGC were also varied with both 3000g and 5000g samples being tested. Figure 3-0-a shows the results of the SGC tests relative to the Modified Proctor density curve. The different sample sizes were used to simulate the different lift heights in the field. The 3000g and 5000g sample sizes are equivalent to 10.2 cm and 15.2 cm lift heights, respectively. At approximately the same water content, the 3000g sample after 800 gyrations reached a higher density than the 5000g sample at 800 gyrations. It was determined from the data that the compacted height of the 3000g sample was approximately 8 cm as opposed to the 13 cm height obtained with 5000g sample. Through a comparison of density to number of gyrations, shown in Figure 3-0-b. Compaction Comparison of 3000g and 5000g Samples, it was observed that a smaller lift height resulted in greater compaction efficiency during field compaction. Given the results, it was apparent that a much larger number of gyrations would be necessary on a 5000g sample size in order to reach a specified density. Therefore, it was determined that smaller lift heights during construction would create a better compacted soil resulting in a runway/taxiway less prone to failure. As a result, it was recommended that at a minimum the top layers of the subbase for CC5 would be compacted at smaller lift heights of 10 cm.

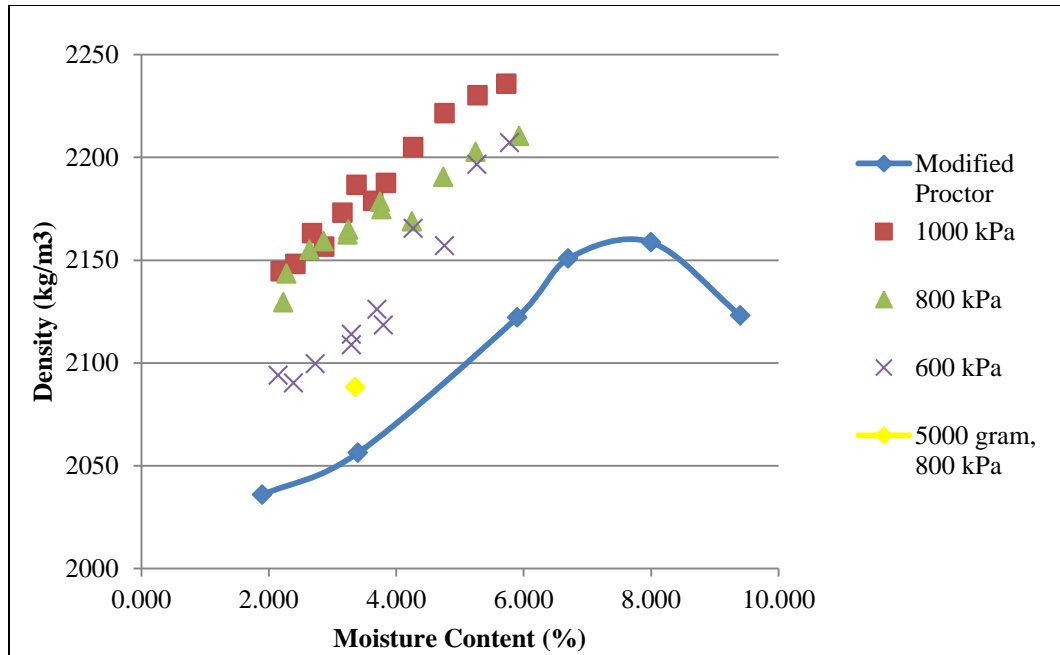


**Figure 3-0-a. Evaluation of P-154 Results below OMC**

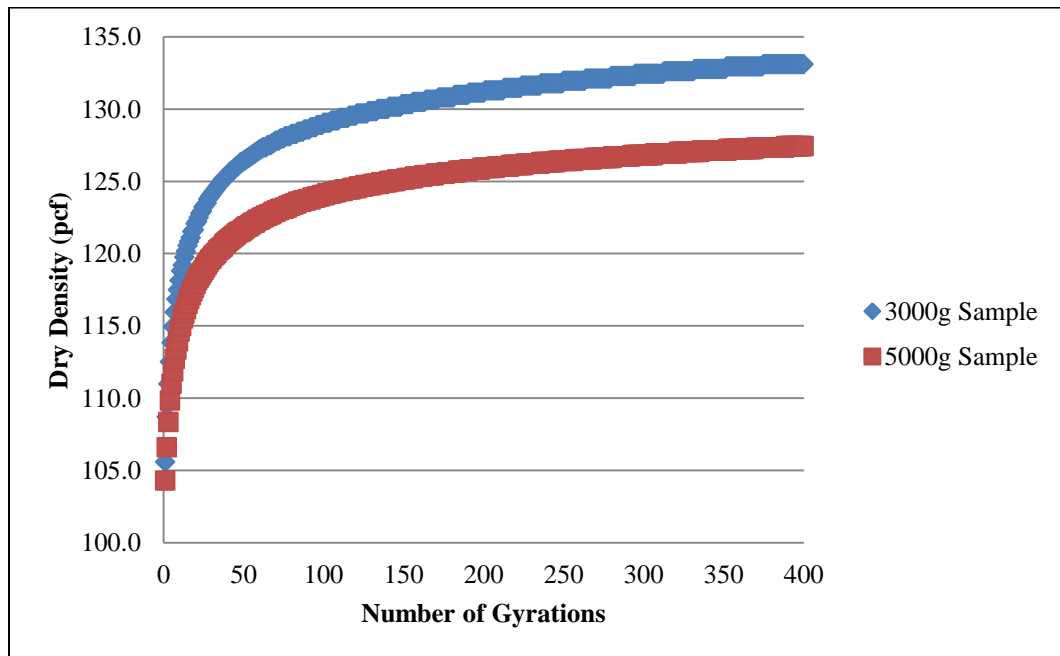


**Figure 3-0-b. Compaction Comparison of 3000g and 5000g Samples**

Since the maximum density achieved with the Modified Proctor test changes with moisture content, SGC tests were also conducted at various moisture contents to observe

its effect on density. The tests were run on 3000g samples at 600, 800, or 1000 kPa for 800 gyrations. A set of tests were run at each moisture content range to provide repeatable results. The displacement achieved for each of the samples followed the same trend as the densities shown in Figure 3-0-a. The final displacements were precise within a tolerance of approximately 0.38 cm and lead to a coefficient of variance of 0.03, showing the repeatability of the SGC testing. The largest displacement for 2-3 percent moisture content tests was approximately 1.71 cm, while the largest displacement for the 6-7 percent moisture content tests was roughly 2.12 cm. The displacement increase for each moisture content is due to excess water acting as a lubricant for the aggregate allowing them to shift with less effort. This allows the SGC to compact the material more completely, leaving less void space amongst the aggregates and therefore maximizing compaction. Unfortunately, as stated in the previous chapter, a substantial amount of drainage, within the upper lifts of the subbase, was observed past a moisture content of 4 percent. However, based on results shown in Figure 3-0-a, dry densities higher than the maximum Modified Proctor density are possible even at the lower moisture contents. It was also determined and shown in Figure 3-0-a that maximum Modified Proctor density could be reached at 4 percent moisture content. Therefore, a recommendation was made to the FAA, mentioned in Chapter 2, to perform all field compaction at moisture contents of 4 percent or less. The results show that due to an increase in confining pressure and moisture content, the gyrations required to reach a specific range of density are significantly decreased, further confirming the SGC's ability to mimic current testing standards while provide greater compacting ability.

Table 3-0-b shows the average number of gyrations needed to reach a specific density range. This table is a summary of all the data that has been accrued throughout the project. It shows the trends and repeatability of the testing. It also backs up Figure 3-0-a by showing that dry density values higher than the maximum modified Proctor density are possible at relatively low moisture contents. The table's main purpose was its use in conjunction with field compaction data to obtain a correlation between SGC lab data and field data that will be discussed further in Chapter 4.

**Table 3-0-b. P-154 SGC Resultant Data**

<b>Pressure (kPa)</b>	1000	800	600	1000	800	600	1000	800	600
<b>Average Moisture (%)</b>	2- 2.5	2-2.5	2-2.5	2.5-3	2.5-3	2.5-3	3-4	3-4	3-4
<b>No. of Tests</b>	2	2	2	1	2			2	2
<b>% Maximum Mod. Proctor</b>	<b>Average Number of Gyrations</b>								
<b>80 - 85%</b>	2	2	4	2	3	-	-	4	6
<b>85 - 90%</b>	8	7	17	8	11	-	-	11	17
<b>90 - 95%</b>	39	43	131	34	44	-	-	39	93
<b>95 - 100%</b>	433	438	517	344	436	-	-	324	481
<b>&gt;100%</b>	-	-	-	717	-	-	-	693	-

Gradation analyses according to ASTM C136 were conducted on loose and compacted P-154 to evaluate the change in gradation due to crushing of material in the SGC. In order to produce accurate values for the fine material, the wash-sieve method, ASTM C117, was implemented. The gradation analysis was first completed on the loose material to produce a baseline for the investigation. The baseline material was then compacted at 1000 kPa for 3200 gyrations to obtain a compacted material for evaluation. It was

determined after the test that gyrations past the 1600 count produced a miniscule amount of compaction. The confining pressure chosen is the highest pressure produced by the SGC. It was decided to use this confining pressure to more accurately simulate the methods of compaction seen in the field, as this analysis was also compared to field data in Chapter 4. The analysis of this material produced a 4-5 percent increase in fines. Figure 3-0-c illustrates the shift in the gradation curve produced between the loose and compacted gradation analyses.

Upon further analysis, the increase in fine material indicates that attrition and abrasion of the aggregate took place during trafficking and compaction in the SGC (Ramamurthy et al., 1974). Attrition and abrasion of the material contributes to the rounding of aggregates, which can reduce interlock and increase the tendency of the aggregate to move into a denser, more closely spaced packing. However, the shift to the right also suggests that some fracture of the larger particles takes place during compaction. A comparison of this data to trafficking material analysis was completed in Chapter 4 to determine the SGC's ability in predicting construction compaction's effect on the morphology and size gradation of the aggregate.



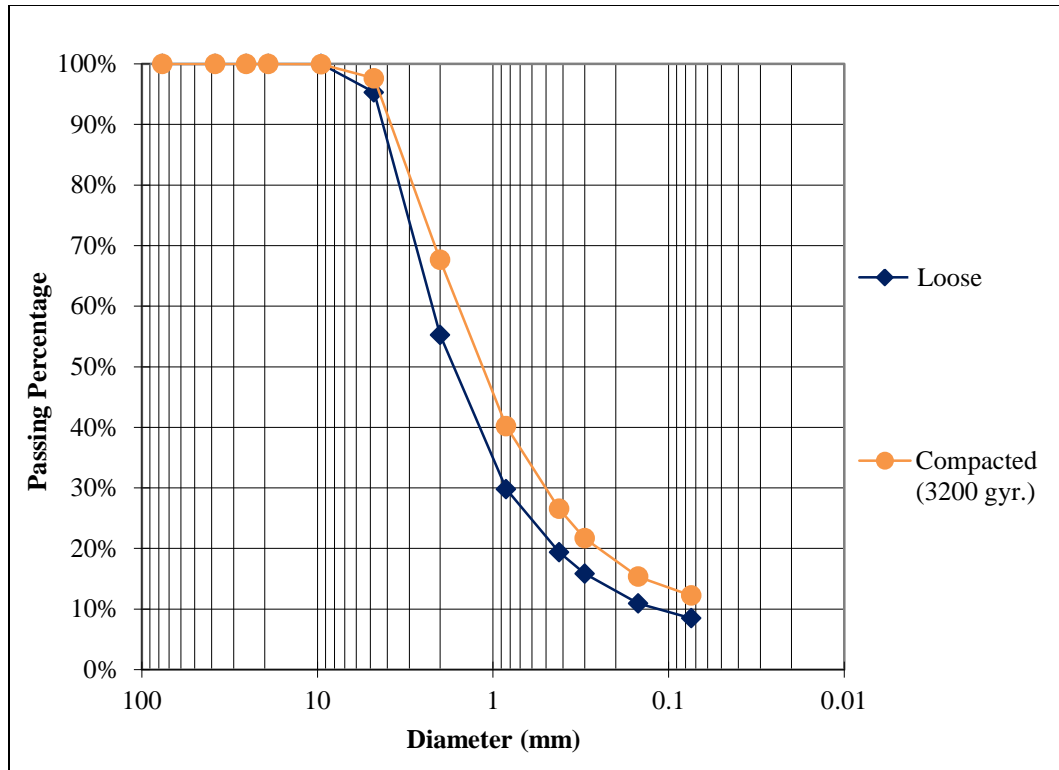


**Figure 3-0-c. P-154 Gradation Analysis**

### 3.3 P-209 Laboratory Experiment Results

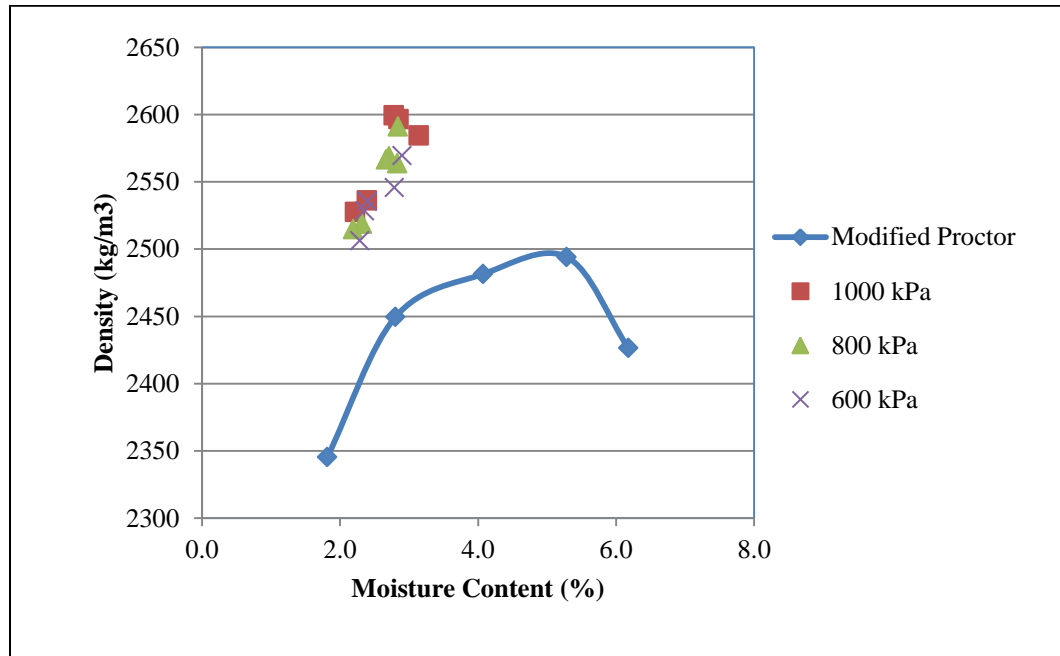
Many of the testing procedures performed on the P-154 were repeated for P-209. Once again, before any SGC tests were run on the P-209 material, Modified Proctor tests (ASTM D-1557) were performed on the P-209 to obtain the optimum moisture content and maximum Modified Proctor density. However, 56 blows per layer and a larger mold, 0.075 cubic feet of volume, were used due to the larger aggregate size. All other parameters of the Proctor test remained consistent with the P-154 Proctor tests, mold size and blows per layer.

Multiple SGC tests were run on the P-209 to study the displacement and obtain repeatability at various moisture content ranges. The P-209 tests were run at three

different confining pressures of 1000 kPa, 800 kPa, and 600 kPa, each with 800 gyrations. All sample sizes remained at a constant 3000g to simulate a 10.2cm lift height like that seen in the field. This standard field lift height was chosen based upon the earlier study with P-154 showing that a larger lift height resulted in a significant decrease in densification. One of the first observations with the P-209 was that it seemed to be unable to retain moisture during the test. This is largely a result of the gradation of the P-209 material being relatively coarse. It was determined that the larger particle size created more paths for moisture migration. This was primarily a problem with moisture contents higher than 3%. As a result, P-209 was tested at lower moisture content than the OMC. Consequently, the highest moisture content used during testing of the P-209 was approximately 3 percent. It was determined through test runs that anything higher would create a moisture migration issue.

As testing data was compiled, it was apparent, just as with P-154, that the tests were repeatable. Results showed that displacement and density for all tests at respective moisture contents and pressures had a coefficient of variance equal to 0.07. This gave promise that the SGC would be a tool that could be used for many types of soils. As expected, the P-209 showed a significant increase in density with increases in moisture content; this is illustrated in Figure 3-0-d. The increase in density with increase in confining pressure was negligible. It was determined that with the P-209 a density higher than that of the maximum Modified Proctor was easily obtainable using the SGC. P-209 was constructed at moisture contents close to 1.5 percent during Construction Cycle 5.

Consequently, the moisture migration issue seen in the SGC did not prove to be an issue during field-to-lab comparisons.

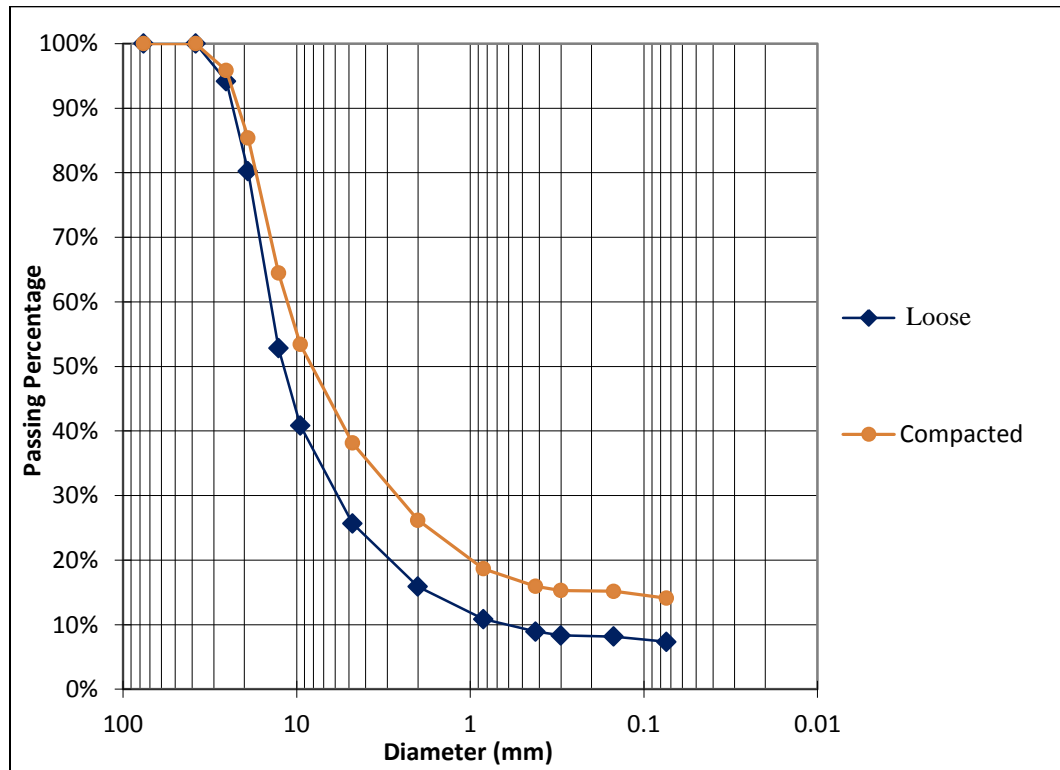


**Figure 3-0-d.** Evaluation of P-209 Results below OMC

All data from P-209 testing were compiled into a tabular format. A portion of these data can be seen in Table 3-0-c. The results show that the final achieved compacted density is not significantly impacted by an increase in confining pressure but shows a significant dependence on moisture content.

**Table 3-0-c. SGC Results for P-209 Field Compaction Comparisons**

Pressure (kPa)	1000	1000	800	800	600	600
Moisture (%)	2.0 - 2.5	2.5-3.0	2.0 - 2.5	2.5-3.0	2.0-2.5	2.5-3.0
No. of Tests	2	2	3	3	3	3
% Maximum Mod. Proctor	Average Number of Gyations					
80 - 85%	29	11	20	15	19	17
85 - 90%	84	34	72	52	70	59
90 - 95%	273.5	124	299	196	308	237
95 - 100%	612	499	643	556	653	591
100 - 105%	-	-	-	-	-	-

**Figure 3-0-e. P-209 Gradation Analysis**

In order to define the modes of grain breakage, gradation analyses were performed on loose P-209 and compacted P-209. A wash-sieve was again completed for each test to acquire an accurate representation of the fine material. The gradation analysis was

completed on the loose material to produce a baseline. The loose material was then compacted at 1000 kPa for 1600 gyrations to obtain a compacted material for evaluation. In this case, 1600 gyrations were used based on the diminishing returns seen past this count in the earlier P-154 testing. The analysis of the compacted material produced a 6-7 percent increase in fines, suggesting that the mechanism of compaction was more abrasion and attrition than fracture. The gradation curves seen in Figure 3-0-e show the results for each material. As with the P-154, the increase in fine material indicated that attrition and abrasion of the aggregate occurred during compaction in the SGC and trafficking. However, the uniform shift to the right for the entire curve suggests that there was a change in grain size at various size ranges indicating that there was also fracturing of the material. Therefore the mechanism of compaction was a combination of attrition, abrasion and fracture.

There are other means of analyzing breakage of material during compaction. For instance, the P-209 material had a much coarser gradation than the P-154 material; consequently, it lent itself to a flat and elongated particle test, described in ASTM D4791. This testing was useful in determining the change in particle morphology characteristics due to compaction. The testing standard requires the use of only the material retained on the 9.53mm sieve. Additionally, for the particles in a particular sieve to be tested, the particle count in that sieve needs to be greater than 100. This limited all testing of P-209 material to the 9.53mm and 12.7mm sieves. Figure 3-0-f represents the data drawn from the 9.53mm sieve for loose and compacted materials. Figure 3-0-g represents the same data for the latter sieve size.

The data for both sieve sizes tend to show a decrease in flat and elongated particles for the compacted material. It can be seen that the 1:1 particles increase in each of the sieve sizes. This was attributed to the fracture of the longer particles along their weak axes such as the 5:1 and 4:1 ratios and also the attrition of the shorter particles such as the 3:1 and 2:1 ratios. The fracture would cause the 5:1 and 4:1 particles to break up into smaller and shorter particles that would be considered 3:1 or lower. The attrition would break the corners of particles rounding them into a ratio closer to 1:1; hence the increase in 1:1 particles after compaction. This supports the theory that fracture was also a method of compaction during compaction. Additionally, the fracture produced sharp edges that were easily broken by attrition or rounded by abrasion.

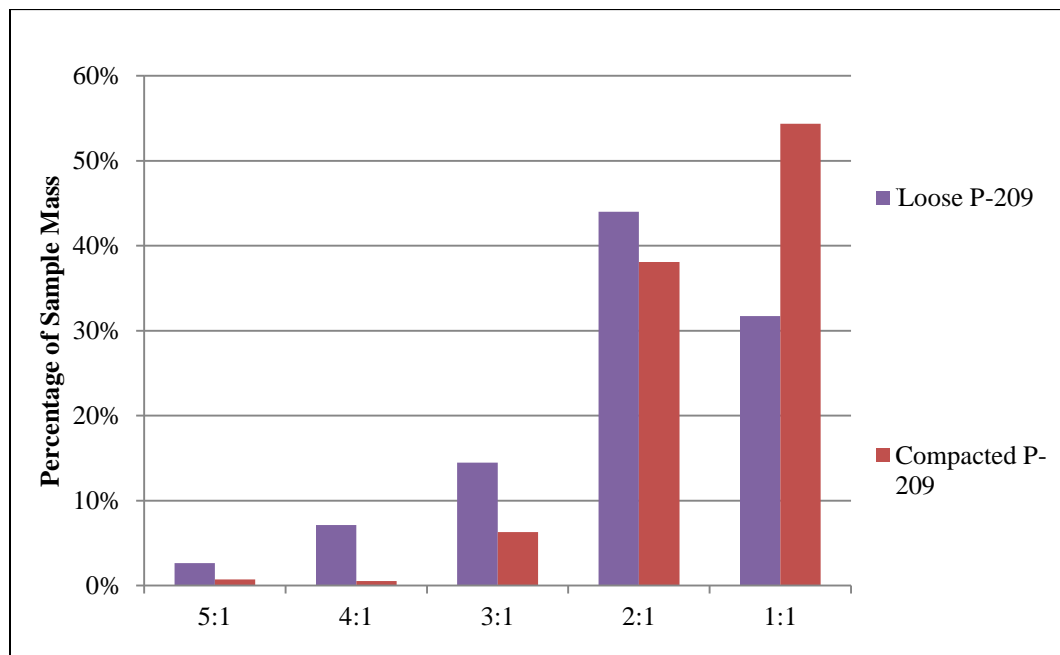


**Figure 3-0-f. P-209 Flat and Elongated on 9.53mm Sieve**

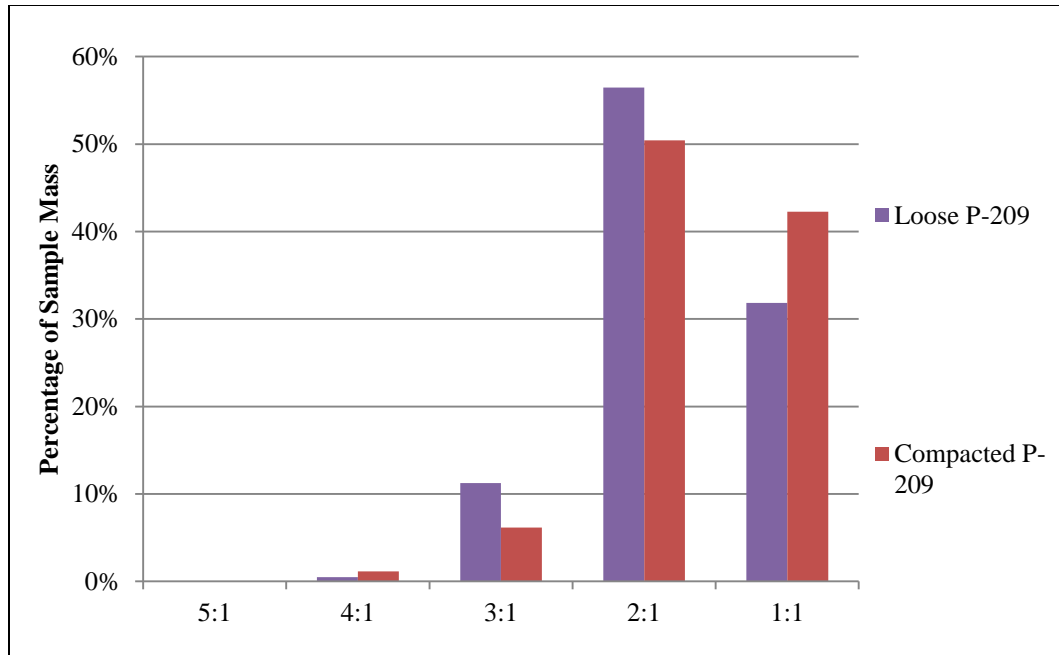


**Figure 3-0-g. P-209 Flat and Elongated on 12.7mm Sieve**

### 3.4 DGA Laboratory Experiment Results

Modified Proctor tests, ASTM D-1557, were performed on the DGA at different moisture contents to find the optimum moisture content and maximum modified Proctor density.

The tests were run to the identical specifications used in the P-209 testing due to the similarly coarse gradation of the DGA. The Proctor curve was plotted against the SGC results in Figure 3-0-h. The DGA behaved similarly to the P-209 when compacted in the SGC due to a similar gradation. Densities above the maximum modified Proctor density were obtained at much lower than optimum moisture content. Water retention mimicked the results of P-209. This meant that if the moisture content of the sample was greater than 3%, the water would seep out of the compaction mold.

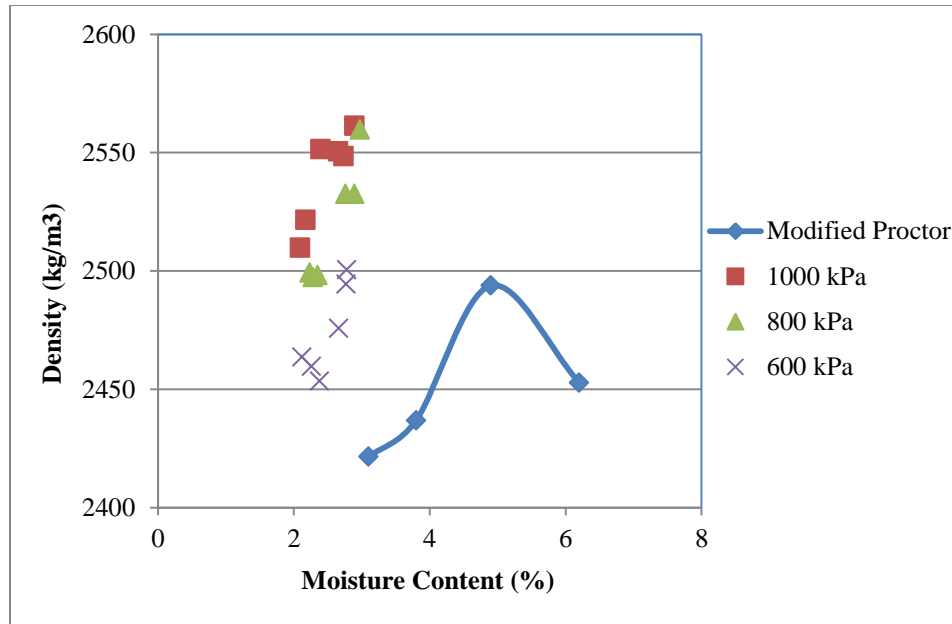


**Figure 3-0-h.** Evaluation of DGA SGC results Below OMC

As with the P-154, SGC tests were run at different moisture content ranges and confining pressures to study the effects that a change in those parameters would impose on the compaction. Many tests at varying moisture contents, gyrations, and confining pressures were run to complete **Table 3-0-d**.

**Table 3-0-d** shows the effects that these variables have on compaction of the DGA. It is apparent that the data is repeatable and shows the trend of increasing densities with moisture content and confining pressure. The contents of this table will be crucial during the development of a correlation table from the SGC to field compaction methods.



**Table 3-0-d. SGC Results for DGA Field Compaction Comparisons**

<b>Pressure (kPa)</b>	1000	800	600	1000	800	600
<b>Average Moisture (%)</b>	2-2.5	2-2.5	2-2.5	2.5-3	2.5-3	2.5-3
<b>No. of Tests</b>	3	3	3	3	3	3
<b>% Mod. Proctor</b>	<b>Average Number of Gyrations</b>					
<b>80 - 85%</b>	4	8	11	1	2	4
<b>85 - 90%</b>	15	26	38	7	10	18
<b>90 - 95%</b>	58	99	161	31	46	88
<b>95 - 100%</b>	295	462	531	172	269	473
<b>&gt;100%</b>	648	784	-	547	632	-

It can be seen that the majority of the compaction occurs within the first 50 gyrations, followed by minimal gains after 100 gyrations.

In an attempt to determine what is happening to the gradation of the DGA during compaction, dry and wet sieving of the material was performed before and after compaction in the SGC. Figure 3-0-i illustrates the sieve analyses performed on the DGA material. The figure illustrates a fairly uniform shift to the right but there is relatively large discrepancy between the two curves at the smaller particle sizes. This implies that the larger particles are not cracking but instead are becoming more rounded. Abrasion occurring during the tests would account for the increase in fines that were observed during the sieve analysis.

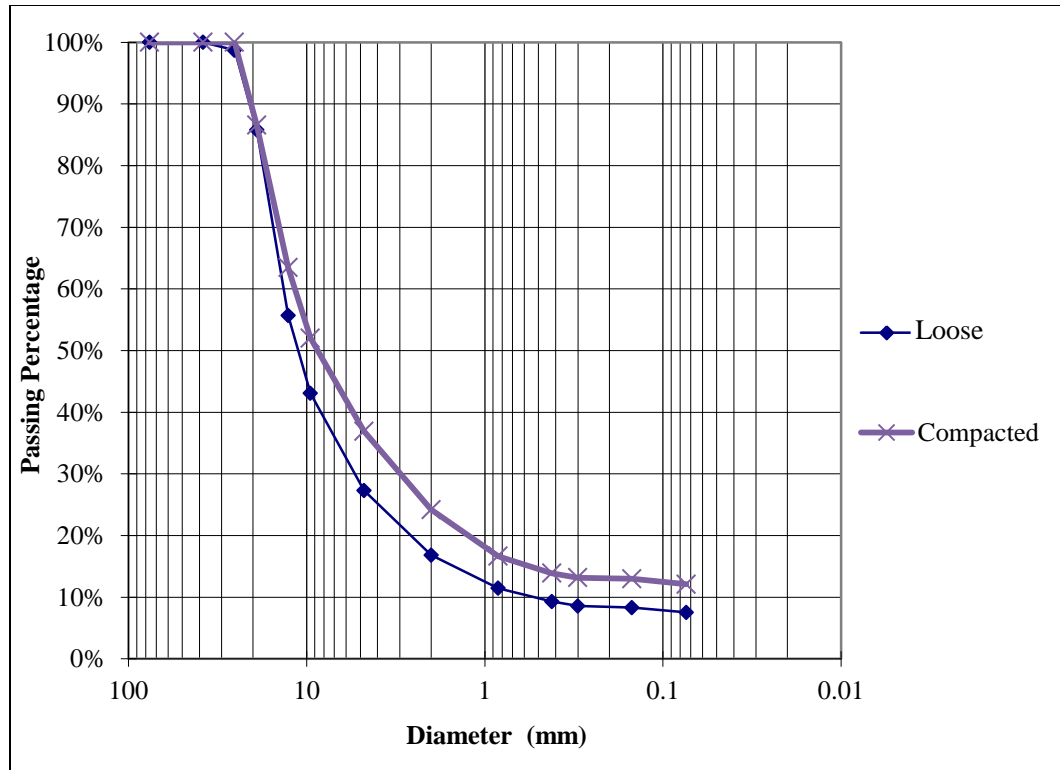


**Figure 3-0-i. DGA Sieve Analysis**

Due to its coarse gradation, similar to the P-209, the DGA was a great candidate for flat and elongated testing. Sieve sizes of 9.53mm and 12.7mm mesh were used due to the lack of aggregate on any sieves with larger mesh. The amount of flat and elongated particles diminished after compaction in the SGC with an increase in 1 to 1 particles. This meant that the compaction in the mold was causing fracture and attrition within the particles. Therefore, the compaction methods of the SGC were repeated on various materials, meaning the compaction method was a combination of attrition, abrasion, and fracture. Due to the extensive testing in this area, it was assumed that this compaction method would be repeatable on many materials and not just the few tested in this study. Results for the flat and elongated testing are shown in Figure 3-0-j and Figure 3-0-k.

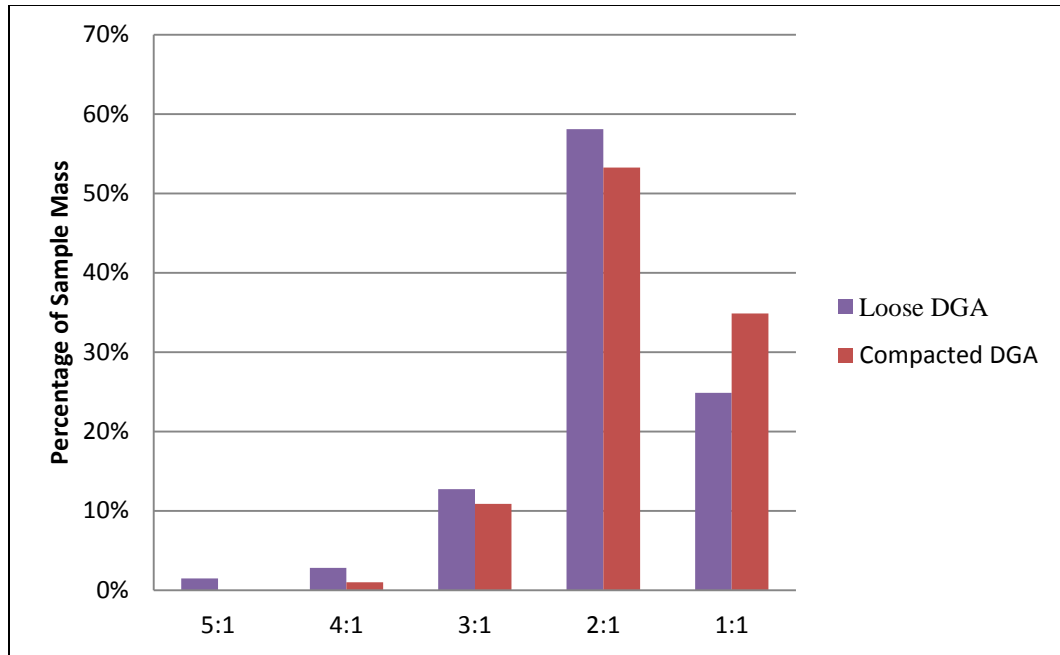


**Figure 3-0-j. DGA Flat and Elongated on 9.53mm Sieve**

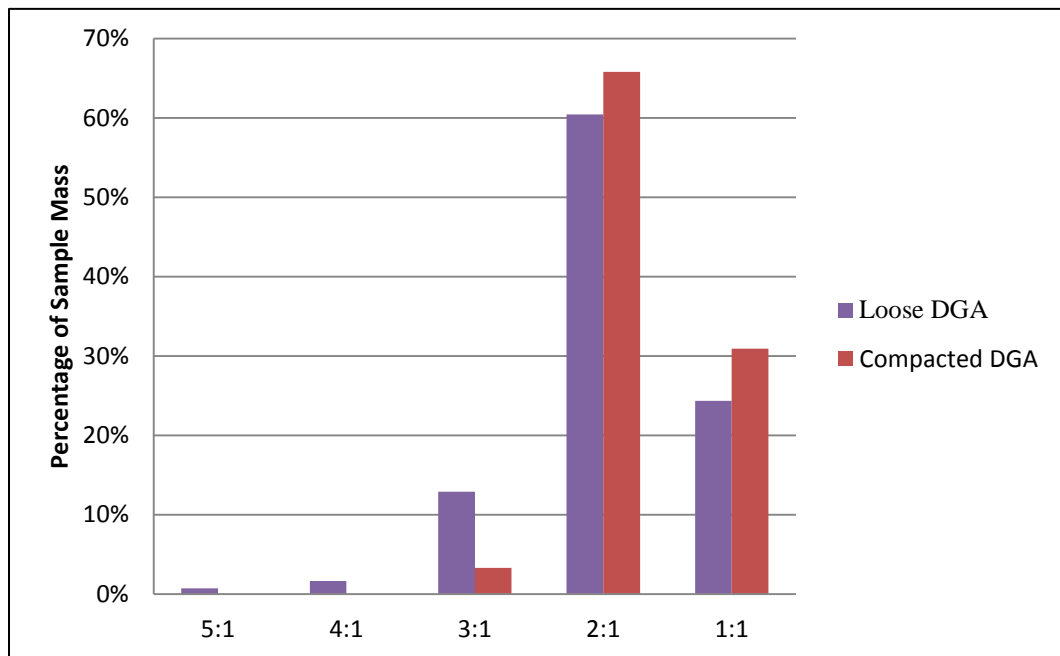


**Figure 3-0-k. DGA Flat and Elongated on 12.7mm Sieve**

### **3.5 SGC Compaction Curve Comparison**

Compaction curves can tell a lot about the behavior of a material during a test.

Compaction curves for each of the materials at 600, 800, and 1000 kPa were developed using a wide range of moisture contents. Figures Figure 3-0-l, Figure 3-0-m, and Figure 3-0-n are examples of these compaction curves. Each of the figures shows the compaction curves for the 2-2.5% moisture content range. Given the side by side comparison, it is simple to see the effects of confining pressure on final dry density. The P-154 material saw the most significant difference with increased confining pressure. The P-209 and DGA saw a less significant increase in density with confining pressure. This was a result of the tighter gradation of those materials. Because of the increase in contact points between aggregate, it takes more energy to compact. Therefore, a significant increase in energy was necessary to see a large jump.

However, the more uniform gradation of the P-154 material creates fewer contact points and therefore less energy is needed to break those contact points and cause compaction. Consequently, the increases in confining pressure resulted in a noticeable increase in density. However, the poor gradation of the P-154 also meant that even at maximum density there would be a large amount of void space between aggregates. This made it impossible to reach maximum modified Proctor densities at low moisture contents with this material.

On the other hand, the well-graded DGA and P-209 materials were left with less void space at final density. The better gradation allowed it to pack more tightly and create a

larger final density. The end result was a final density for each of these two materials larger than the maximum modified Proctor density, even at lower than typical moisture contents.

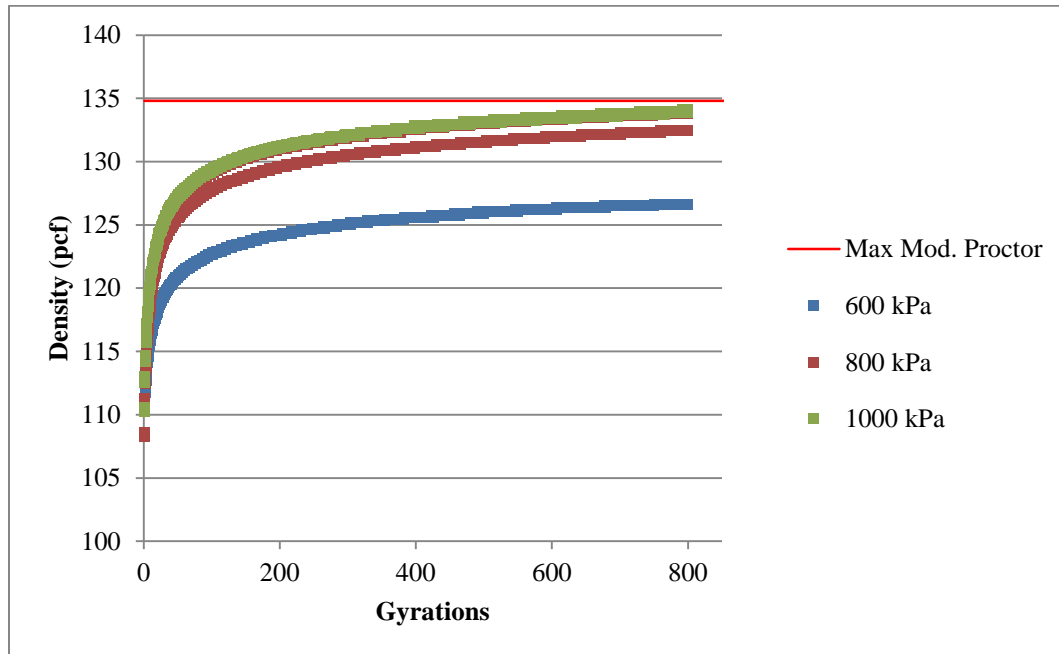


**Figure 3-0-l.** Compaction Curves for P-154 at 2 to 2.5% moisture content range

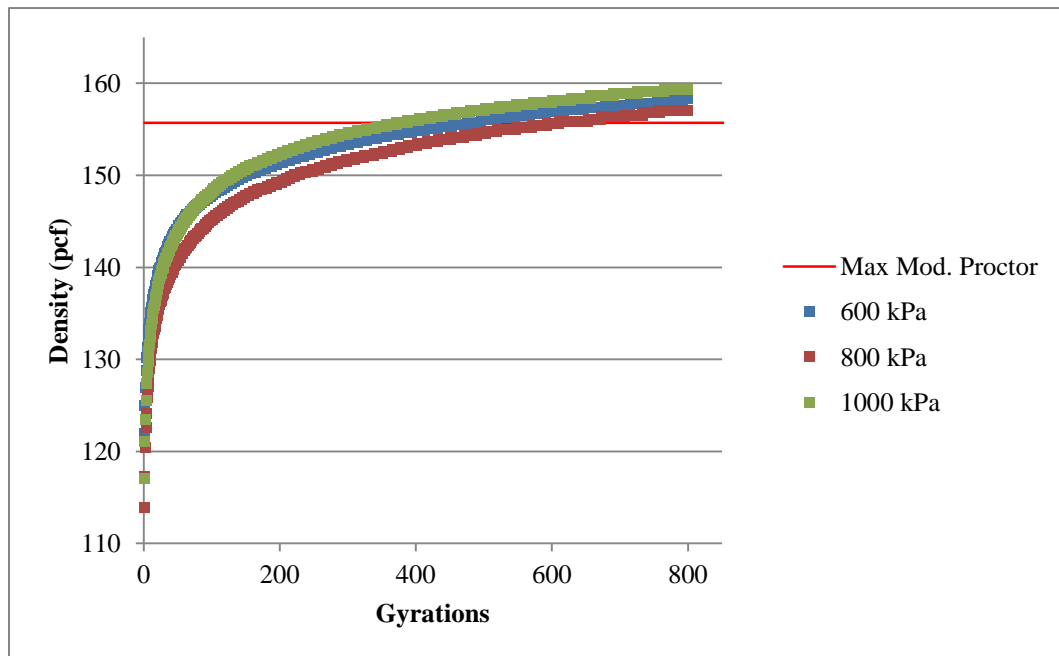


**Figure 3-0-m.** Compaction Curves for P-209 at 2 to 2.5% moisture content range

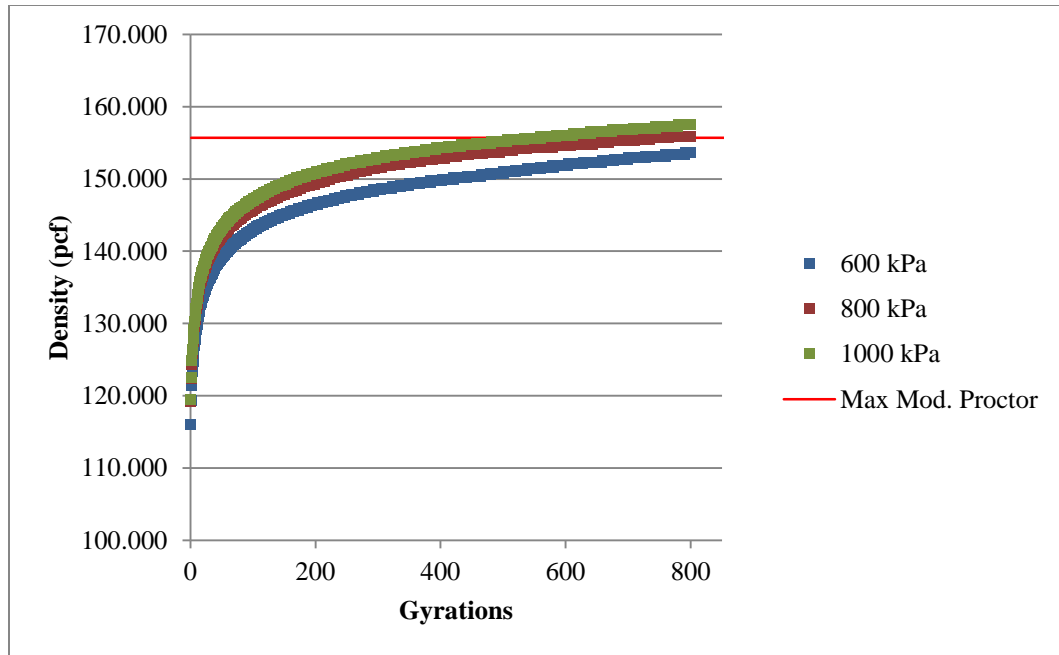


**Figure 3-0-n.** Compaction Curves for DGA at 2 to 2.5% moisture content range

### 3.6 Energy Measurements

In order to study the energy input during compaction, a pressure distribution analyzer was used during testing. The energy input consisted of both shear work and vertical work.

Due to the gyrations of the machine, the shear work data contains many short spikes. In an attempt to eliminate these discrepancies the shear work was zeroed, which allows for a standard at which the pressure distribution analyzer, PDA, was leveled and not jammed against the mold. This also eliminated the first 10 gyrations during which the majority of the work done was vertical work.

Figure 3-0-o contains the sum of the vertical, shear and total work for P-154 during 800 gyration tests. The figure shows that as moisture content increased, the sum of the vertical work done on the sample increased. This was a result of lubrication properties of water within the aggregate allowing them to rearrange with less effort to reach a denser

state. This denser state resulted in a greater vertical displacement of the sample, which is directly proportional to vertical work. The figure also showed that as moisture content increases the sum of the shear work on the sample decreases. This is a result of the greater moisture content allowing the aggregates to be arranged into a denser state with less energy. Ordinarily, the aggregate will require a certain amount of shear work to reach this dense state. However, since the higher moisture content allows the aggregate to be rearranged more easily with vertical work, the amount of shear work necessary to reach this dense state was reduced. The same trend is also shown in the sum of the total work, as moisture content increases the sum of the total work decreases. Another note worth mentioning is that the shear work comprised the majority of the work, over 100 times the amount of vertical work, making vertical work negligible.

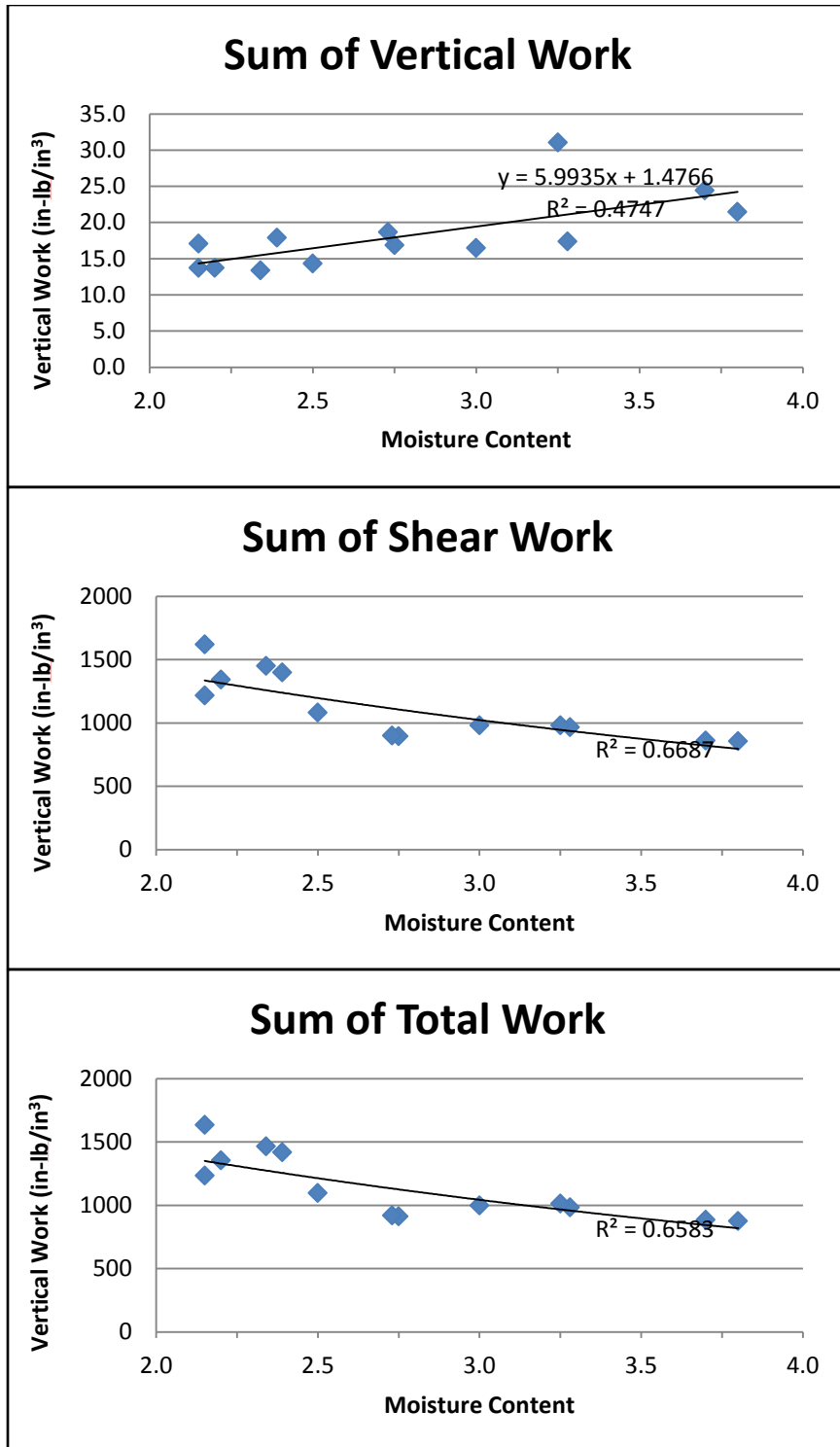


**Figure 3-0-o. P-154 Energy Measurements**



Similar tests were performed on P-209 and the energy results are displayed in Figure 3-0-p. The energy measurements for P-209 did not create a trend and showed much more scatter in the results. This was more than likely a result of the coarser gradation of P-209. The SGC mold was not large enough to produce a representative sample. More tests were planned to confirm the energy measurements for P-209. However, at the time of this study those tests had not been completed. P-209 does show a trend similar to P-154 in that the major component of the work done was a result of shear work.

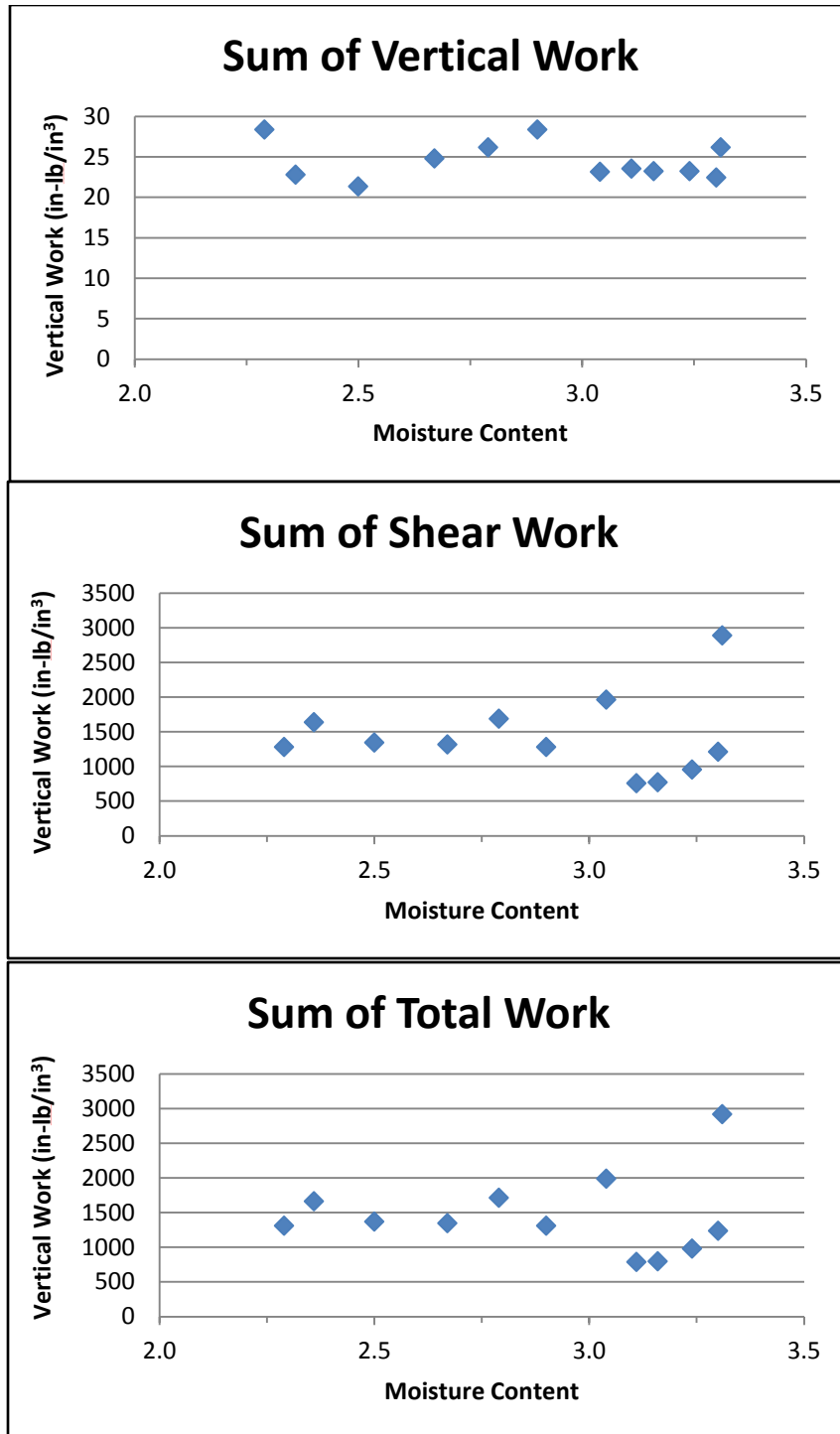


**Figure 3-0-p. P-209 Energy Measurements**

The sum of each component of energy for P-154 and P-209 were compared as can be seen in Figure 3-0-q. Though there was no clear trend for P-209, it appeared that there

was more energy input into the P-209 sample than the P-154. This was a result of the more uniform gradation of P-209 which required more energy to compact because of better aggregate interlock.

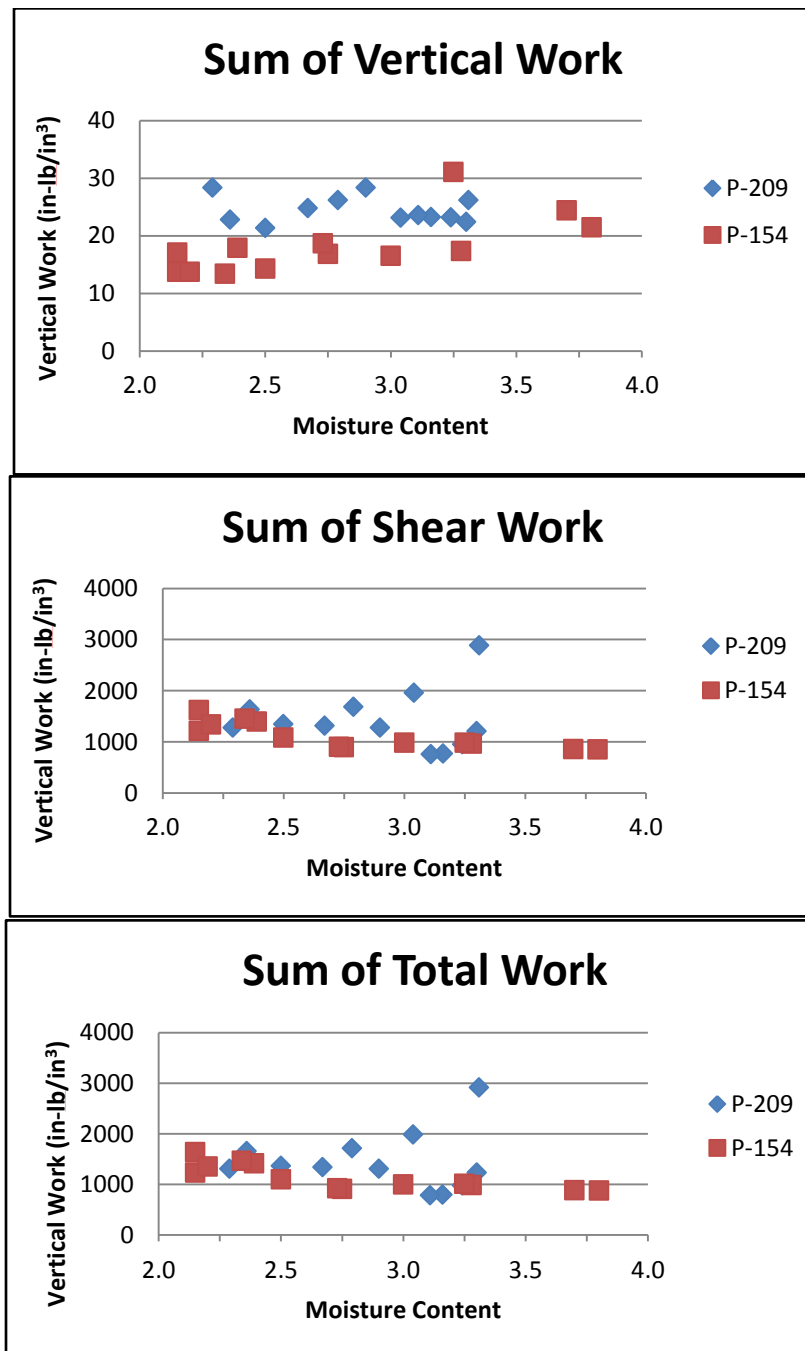
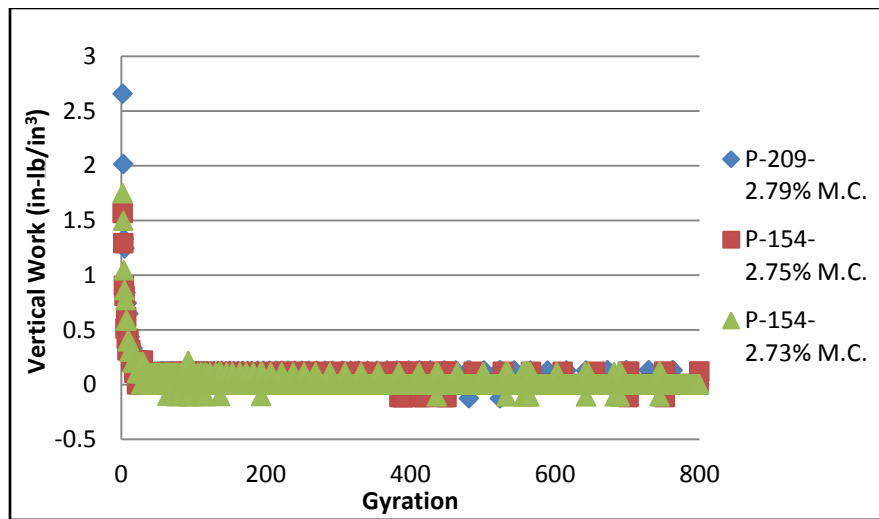


Figure 3-0-q. Sum of Energy Material Comparison for P-154 and P-209

A comparison of the energy measurements per gyration in the SGC was also completed. The vertical work was measured for each material at various moisture contents. Figure 3-0-r illustrates the trend seen for a moisture content of 2.7 to 2.8 percent. All moisture contents showed an identical trend and only differ in the quantitative values of work done. Recall that the majority of compaction takes place in the first 50 to 100 gyrations. Since vertical work and compaction go hand in hand, the bulk of vertical work was performed in the first 50 gyrations and leveled off shortly thereafter. Because the compaction curve and the vertical work curve were directly proportional during the first 50 gyrations, it was observed that the first 50 gyrations was mostly vertical work and very little shear work.



**Figure 3-0-r.** Vertical Work per Gyration at 2.75% M.C. for P-154 and P-209

A similar comparison was made for the shear work per gyration. Comparisons were made at 2.50, 2.75, 3.00, and 3.25 percent moisture content. The results of this analysis are displayed below in Figure 3-0-s. There was a significant difference in the shear energy between P-154 and P-209. Oftentimes, the P-154 required much less shear energy per gyration than P-209. This was attributed to the more uniform gradation of P-154

when compared to the well graded P-209. A more uniform gradation leads to less contact points among the particles. Consequently, less energy is required to break the contacts between particles. There is also an apparent cyclic nature to the plots. This is attributed to the rotation of the mold in the SGC changing the location of loading during the gyration. A full cycle on the graph means that the mold made a full rotation in the machine.

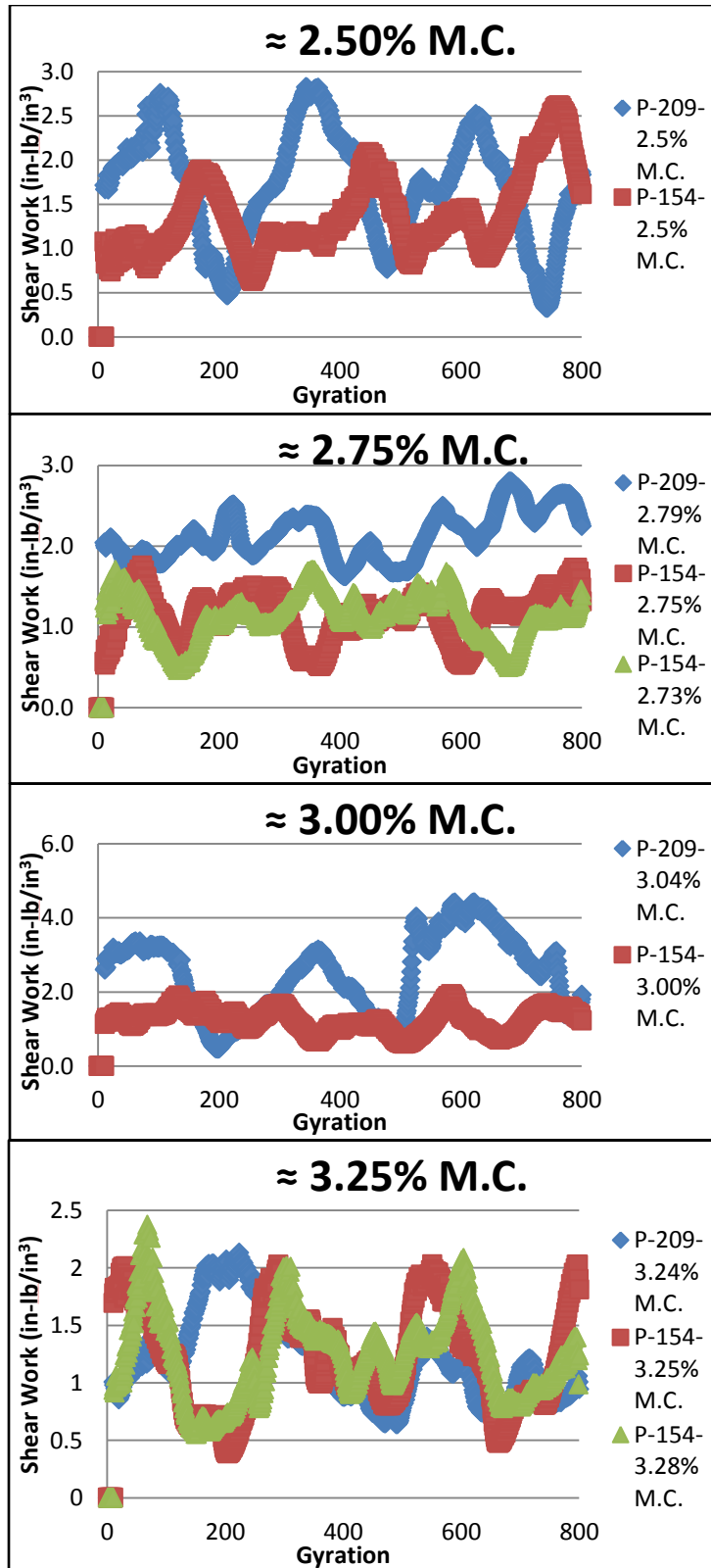


Figure 3-0-s. Shear Work per Gyration Comparison of P-154 and P-209

Additionally, the results of the energy tests were averaged and compiled for further analysis. Table 3-0-e shows the end result of this compilation. It clearly shows that the work done by the SGC on the sample to reach the Modified Proctor density is much lower than the energy input during a Modified Proctor test. The standard measurable energy input of a Modified Proctor test is 56,000 lb-ft/ft<sup>3</sup> (Das, 2010). The SGC was able to reach between 90-95% of the Maximum Modified Proctor density with less energy input and at much lower moisture content than optimum. This made it evident that the SGC was much more efficient than the Proctor methods at compacting the specimen due to the shear work being done on the sample in addition to the vertical work. This finding is similar to the results seen in the field with modern compaction equipment. It also shows that as the moisture content was increased, the work required to reach a specific density was decreased.

**Table 3-0-e. Average SGC Work at 600 kPa to Obtain Modified Proctor Density**

	P209	P209	DGA	DGA	P154	P154	P154
	2-2.5%	2.5-3%	2-2.5%	2.5-3%	2-2.5%	2.5-3%	3-4%
Respective Modified Proctor Density (pcf)	145.3	151.3	143.4	151.2	126.3	126.6	128.4
Maximum Modified Proctor Density (pcf)	155.7		155.8		137.0		
Percent of Maximum Modified Proctor Density	93.3%	97.2%	92.0%	97.0%	92.2%	92.4%	93.7%
Modified Proctor Energy (lb-ft/ft <sup>3</sup> )	56000	56000	56000	56000	56000	56000	56000
Respective SGC Density (pcf)	145.3	151.3	143.4	-	126.3	126.6	128.4
Average SGC Work (600 kPa) (lb-ft/ft <sup>3</sup> )	24219.5	51555	18364.6	-	32627	-	47757
Average SGC Work (600 kPa) to reach lower Moisture Content's Proctor density (lb-ft/ft <sup>3</sup> )	-	22759	-	-	-	-	25914

The results from the PDA will be compared to the compaction energy in the field, once a reliable and accurate method of finding the energy in the field is formulated. Currently, a means of doing this through finite element analysis has been and continues to be explored. Obtaining the compaction energy in the field will allow a precise and accurate correlation between SGC results and number of traffic passes to be obtained for each aircraft.



## Chapter 4

### Field to Laboratory Comparison

#### 4.1 P-154 Field Compaction Results

Field compaction was closely monitored throughout the construction of CC5. Density measurements were taken using one of two methods, a nuclear density gauge or a sand cone. In addition, elevations were recorded. The densities observed during construction were below the maximum Modified Proctor density. This lower density could be attributed to the lower than optimum moisture content used to prevent moisture migration to the subgrade. The results from lifts one, two, and five are shown in **Error! Reference source not found.** along with the results of SGC testing at similar moisture contents. Lift three was excluded because the material used was from a different screening which resulted in a higher maximum Modified Proctor density. Additionally, lift four was completed on two separate days, creating a gap in the data. Therefore, lift four was not used in determining the compaction characteristics and has not been shown for that reason. It should be noted that only six passes of the roller were used on lift one to prevent penetration of the subbase material into the subgrade layer which provided the lowest density of all the lifts.

After a specific number of passes with the roller, the change in height and density were measured at six separate locations within each lift. Because of the discrepancies in the heights and densities, it was more useful to take the average of a series of points for each lift. The data seen in Figure 4-0-a has been averaged to eliminate the discrepancies as much as possible.

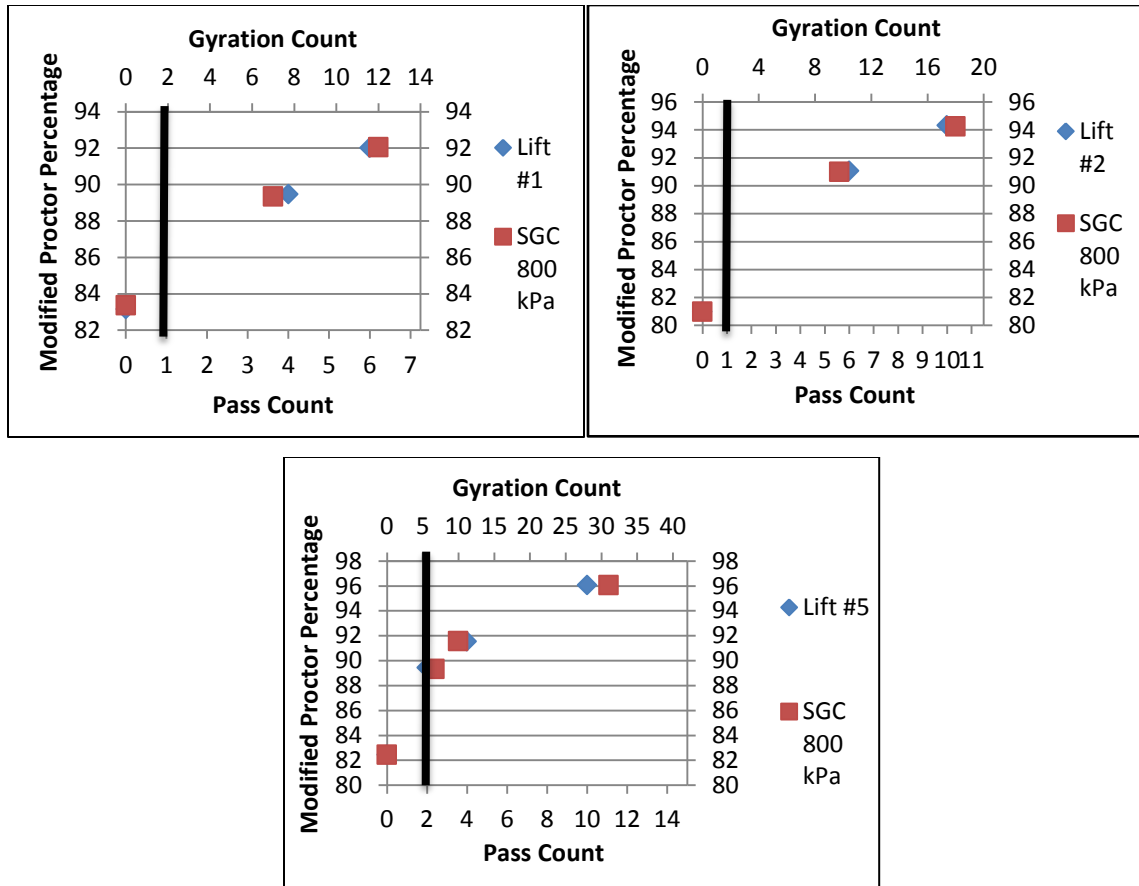


**Figure 4-0-a. P-154 Construction to SGC Density Correlation**

The percent of maximum Modified Proctor density was plotted against the number of gyrations and number of passes of the roller to investigate the correlation between the SGC results and field compaction. The graph shows that the field data can be closely replicated by the SGC at a confining pressure of 800 kPa. A similar trend was seen for each of the lifts. In Figure 4-0-a, a line was drawn from through the horizontal axes to form a correlation of gyrations to roller passes. Lift one and two were compacted with a vibratory steel roller. Figure 4-0-a shows that a vibratory steel roller pass is approximated by two gyrations in the SGC at this confining pressure. This was also observed in lift two.

Lift five was compacted with a vibratory steel roller followed by a rubber tire roller. Regardless of the two different rollers used, lift five was still closely replicated by 800 kPa tests in the SGC. The combination of the rollers resulted in greater densities in lift five, effectively increasing the ratio of passes to gyrations. As a result, a pass when using a combination of rollers is approximately equivalent to three gyrations in the SGC. These correlations along with results from 800 kPa SGC tests suggest that a steel roller would have to complete approximately 60 passes to reach 100 percent Modified Proctor density and a combination would require 40 passes at three percent moisture content. This is due to diminishing returns as the density increases. However, no data exists past 12 passes with the rollers to test this theory. Regardless, 40 to 60 passes per lift would not be feasible. Nevertheless, 20 passes with the combination is more feasible and should obtain a density of about 98 percent Modified Proctor, a density that should greatly increase the life of the pavement.

#### **4.2 P-154 Evaluation of Performance Characteristics**

A gradation analysis was conducted on trafficked material, after roughly 20,000 passes, for comparison to the loose and compacted gradation analyses performed earlier. In order to obtain accurate values for the fine material passing the #200 sieve, the wash-sieve method was used. The material used for the trafficked portion of the evaluation was from the upper most layer of CC5. An analysis of this material produced 4-5 percent more fines than the baseline material, suggesting that the mechanism of compaction is the same as that seen during compaction in the SGC. The gradation curves seen in Figure 4-0-b show the results for each material. The figures show the close relationship and

similar trend of the trafficked and compacted gradation analyses. This further indicates that the gyratory action and pressure in the SGC is well-suited for the evaluation of compaction characteristics of trafficking. This not only backs the SGC's ability to predict densification in the field but also its ability to predict the effect of compaction on the geometry and gradation of the aggregate.

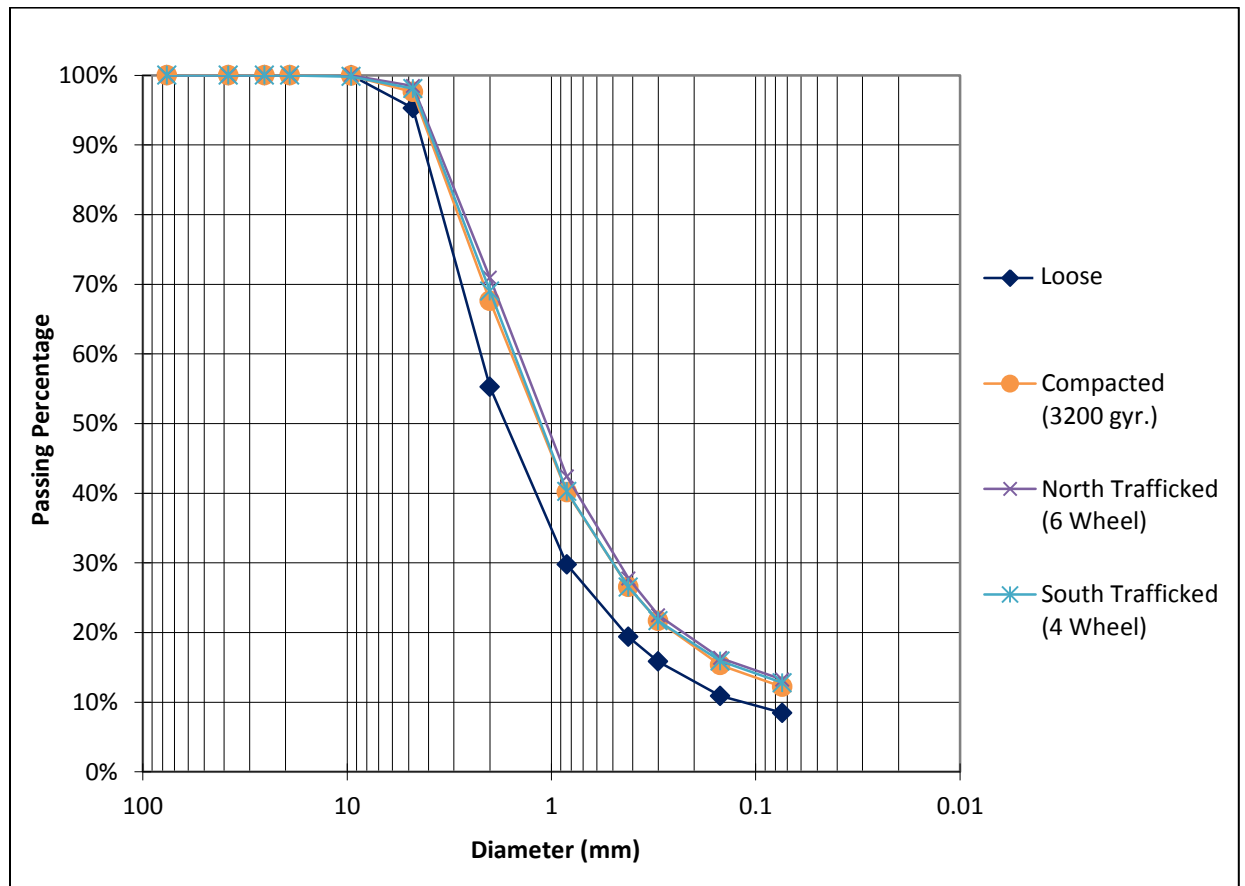


**Figure 4-0-b. P-154 Gradation Analysis Evaluation**

### 4.3 P-209 Field Compaction Results

The percent of the maximum Modified Proctor density was plotted against the number of gyrations and number of passes of the roller to investigate the correlation between the SGC results and field compaction. These tests were performed at similar moisture contents to those used during construction, roughly 1.25%.

Lift one was compacted with a vibratory steel roller followed by a rubber tire roller. Lift two was compacted with two passes of a vibratory roller and two passes of a static smooth roller. The tighter gradation of the P-209 led to similar results regardless of the roller type and configuration. With the SGC compacting at a confining pressure of 800 kPa one pass of a roller translated to ten gyrations in the SGC. These results can be seen in Figure 4-0-c. The information given by this chart can be used to obtain the approximate number of passes required to reach a certain density by simply running an SGC test at 800 kPa.

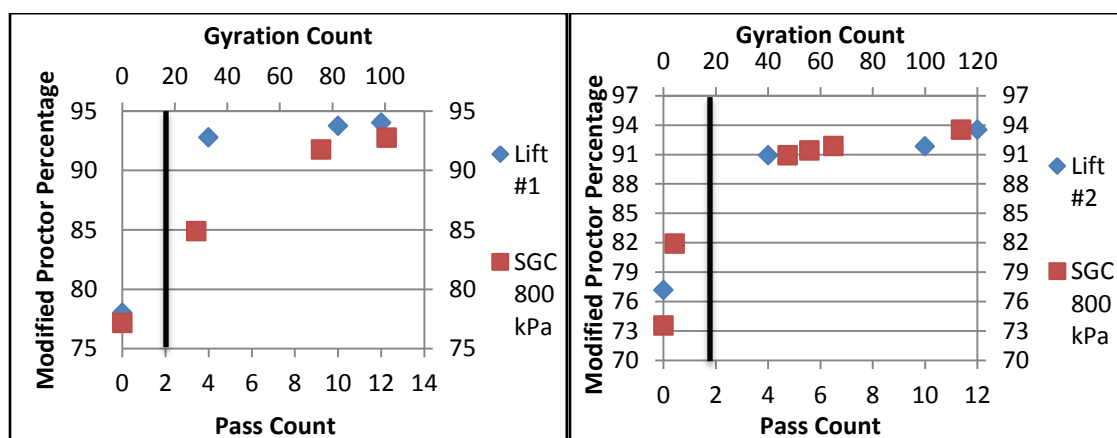
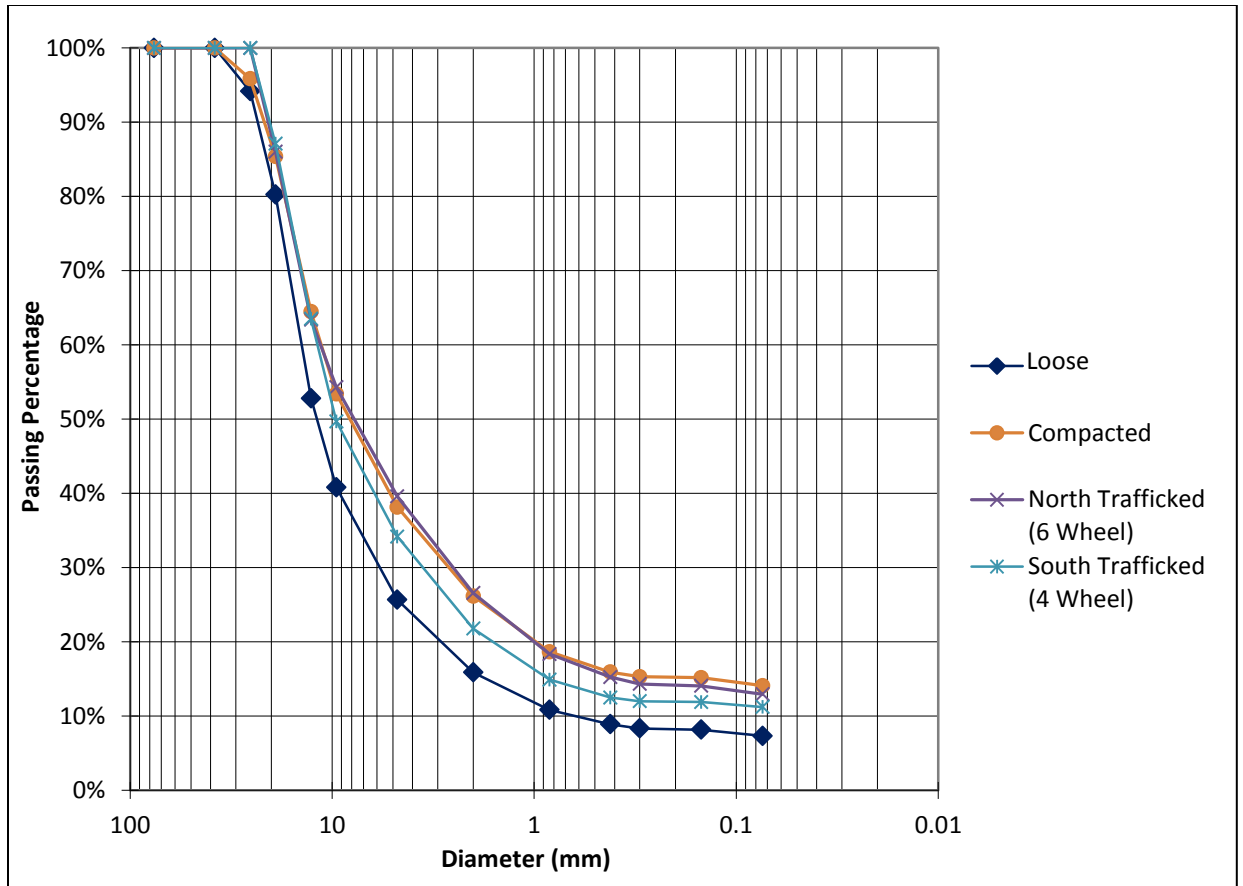


Figure 4-0-c. P-209 Construction to SGC Density Correlation

#### **4.4 P-209 Evaluation of Performance Characteristics**

Additional gradation analysis was performed on trafficked P-209, of roughly 20,000 passes, to evaluate the method of compaction observed during trafficking and compare them to the SGC compaction. A wash-sieve was again completed for each test to acquire an accurate representation of the fine material. The material used for the trafficked portion of the evaluation was from the top of the base layer from CC5. An analysis of the trafficked material produced 4-6 percent more fines than the loose material, which is similar to what was observed with the P-154. Recall that the analysis of the compacted material produced a 6-7 percent increase in fines, suggesting that the mechanism of compaction is similar to that seen in trafficking. The gradation curves seen in Figure 4-0-d show the results for each material. The figure shows the close relationship of the trafficked and compacted gradation analyses. In future testing, more compacted samples will be analyzed. It is expected that an average of compacted samples will create a closer relationship. However, the current curves in Figure 4-0-d suggest that the gyratory action and pressure in the SGC was well-suited for the evaluation of compaction characteristics of trafficking for the P-209 material as well.



**Figure 4-0-d. P-209 Gradation Analysis Evaluation**

Since, the P-209 material lent itself well to a flat and elongated particle test, ASTM D4791, data was obtained for the trafficked material as well. This allowed for a comparison of flat and elongated results from loose, compacted, and trafficked material. Figure 4-0-e shows the data obtained for material retained on the 9.53 mm sieve for trafficked, loose, and compacted materials. Figure 4-0-f represents the same data for the 12.7 mm sieve size.

The data for both sieve sizes tends to show a decrease in flat and elongated particles for the trafficked and compacted material. As with the compacted material, the 1:1 particles increase in each of the sieve sizes. This was attributed to the fracture of the longer

particles such as the 5:1 and 4:1 ratios and also the attrition of the shorter particles such as the 3:1 and 2:1 ratios. The fracture would cause the 5:1 and 4:1 particles to break up into smaller and more than likely shorter particles that would be considered 3:1 or lower. The attrition broke the corners of particles which rounded them into a ratio closer to 1:1. Hence the increased number of 1:1 particles after compacting and trafficking has been completed. As a result, the methods of compaction for trafficked material seemed to mimic that of the SGC, as they were a combination of particle fracture, attrition, and abrasion. Nevertheless, the SGC is able to mimic the compaction methods of landing gear tires due to its gyratory action or shear work.

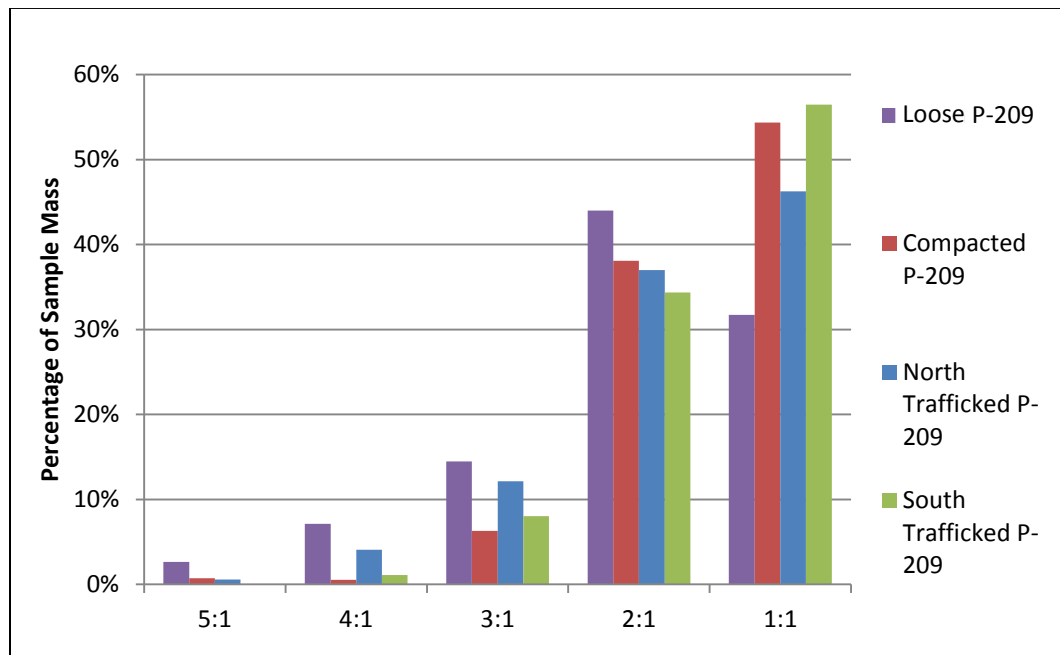


**Figure 4-0-e.** P-209 Flat and Elongated on 9.53mm Sieve



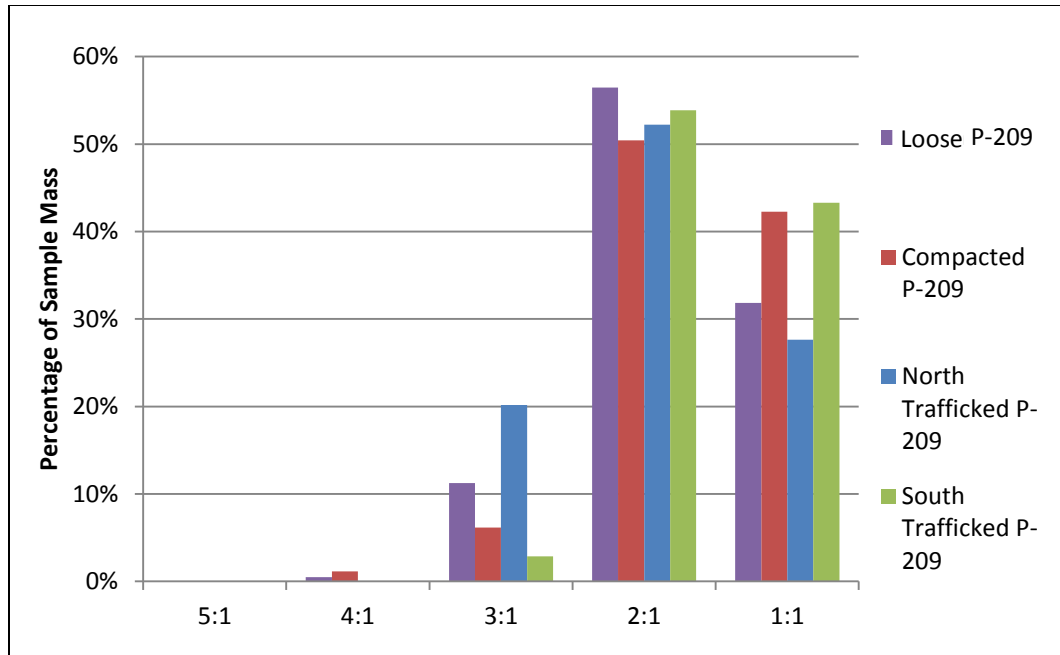


**Figure 4-0-f. P-209 Flat and Elongated on 12.7mm Sieve**

Chapter 4 provides initial comparisons and correlations between the laboratory experiments using the SGC and field construction compaction. Unfortunately, no field data for the DGA material was available for comparison. This study will be expanded in the future to obtain more correlations that could be of great significance during airport pavement design.

## **Chapter 5**

### **Conclusions**

#### **5.1 Summary of Findings**

Based on the extensive research and studies, it is concluded that the SGC is capable of replicating field compaction results for the highly advanced field compaction equipment in use today. It was also capable of achieving much higher densities than the standard energy input of the Modified Proctor test.

Additionally, it was discovered that the SGC has the capability of modeling the behavior of unbound materials in the long term and thereby predicting their performance during compaction and trafficking. This was indicated by a comparison of SGC data with data obtained from the FAA for a six wheel aircraft gear configuration similar to the one used for the B-777. Furthermore, it can be used more effectively than the Proctor tests in providing recommendations about lift heights and achievability of required densities at various moisture contents. This was apparent when the SGC tests were compared to the Proctor density data.

The most significant outcome of this study was the correlation between construction compaction and the SGC. The correlation produced a ratio between the numbers of gyrations in the SGC and the number of passes with a roller. This will provide useful data when attempting to determine the number of passes with a roller necessary to reach a certain density. The mechanism of compaction during trafficking for the aggregate tested is particle rearrangement. However, there was a small amount of compaction due to

attrition, abrasion, and fracture of the aggregate. These methods led to a reduction in angularity and ultimately a decrease in aggregate to aggregate interlock. Additionally, sieve analysis and flat/elongated data was analyzed to determine if the SGC was capable of simulating the amount of attrition, abrasion, and fracture seen during trafficking. The results from the sieve and flat/elongated tests for both the compacted and trafficked material confirmed a very similar type of compaction between the field and the SGC.

## **5.2 Recommendations**

Using the Superpave Gyrotory compactor was the method researched within this study. This method provides a tool capable of replicating field compaction methods within the laboratory. Using this method, correlations between field compaction and experimental compaction have been obtained for typical airport subbase and base types. These correlations can be useful during the construction phase of the airport pavement.

However, the ultimate goal was to determine a correlation between trafficking passes and the SGC. This is one of the shortfalls of this method due to the lack of field data and also the inability to reliably measure energy in the field. A method for estimating compaction energy in the field has to be determined so that it can be used for comparison with the energy input in the SGC. This will enable the SGC tests to be further refined to simulate aircraft trafficking and give the ability to reliably predict pavement performance without full-scale testing.

### **5.3 Future Work**

Future studies in this research will include a further refinement of the correlation between field compaction equipment and the SGC and testing of the correlation between the field compaction and SGC for accuracy and usefulness during the next construction cycle. Additionally, a method for measuring and/or estimating the energy input of the landing gear within the field will be determined. Finally, using this energy measurement method, a correlation of SGC energy with Field energy will be developed after the next construction cycle.

## List of References

1. National Airport Pavement Test Facility. “About the NAPTF”. <<http://www.airporttech.tc.faa.gov/naptf/index.asp>>. 2009.
2. National Airport Pavement Test Vehicle. “About the National Airport Pavement Test Vehicle”. <<http://www.airporttech.tc.faa.gov/naptf/naptv.asp>>. 2009.
3. National Airport Pavement Test Facility. “Construction Cycle 5”. <<http://www.airporttech.tc.faa.gov/naptf/cc5.asp>> . 2011.
4. Advisory Circular, “Standards for Specifying Construction Of Airports”. AC no. 150/5370-10F. N.p.: FAA, 2011. Print.
5. Garg, N., Hayhoe, G. F. Consolidation of aggregate base and subbase layers under heavy aircraft loading at the National Airport Pavement Test Facility. Proceedings of the Advanced Characterisation of Pavements and Soil Engineering Materials, Athens, June 2007.
6. Hayhoe, Gordon F., and N. Garg. “Traffic Testing Results from CC3 Flexible Pavements at the FAA’S NAPTF”. Tech. Atlantic City: n.p., 2006.
7. Dong, M., Hayhoe, G. Analysis of Falling Weight Deflectometer Tests at Denver International Airport. Presented for the 2002 Federal Aviation Administration Technology Transfer Conference, 2002.
8. Timm, David H., and Angela L. Priest. *Wheel Wander at the NCAT Test Track*. Rep. no. 05-02. Auburn: NCAT, 2005. NCAT. Web. 7 Feb. 2013. <<http://ncat.us/files/reports/2005/rep05-02.pdf>>.
9. Microsoft SQL Server 2005. Seattle: Microsoft, 2005. Computer software.
10. Airbus Industrie. LCPC / Airbus/ STBA A380 Pavement Experimental Programme. Toulouse, France. <<http://www.stac.aviation.civile.gouv.fr/publications/documents/rapportPEP.pdf>>. 2001>.
11. Rodway, B., Leigh J., Wickham, G. Interaction Between Wheels and Wheel Groups of New Large Aircraft. Published in Airport Technology Transfer Conference, Atlantic City, U.S.A., Federal Aviation Administration. 1999.
12. Donovan, P. and Tutumluer, E. Analysis of NAPTF Trafficking Response Data for Pavement Foundation Deformation Behavior, FAA Worldwide Airport Technology Transfer Conference and Exposition, Atlantic City, NJ, April .2007.

13. Das, B. Principles of Geotechnical Engineering, Seventh Edition. Cengage Learning. 2010.
14. Swan, C. Class Notes, University of Iowa. 2009.  
<<http://www.engineering.uiowa.edu/~swan/courses/53030/notes/gsd.pdf.53:030>>.
15. Ramamurthy T., Kanitkar V.K., Prakash K., “Behavior of coarse-grained soils under high stresses,” Indian Geotechnical Journal, 4(1), 39–63 1974.
16. US Department of Transportation, Federal Highway Administration. “Pavements”. July 22, 2009.
17. US Department of Transportation, Federal Highway Administration. “Bituminous Mixtures Laboratory”. 2009.  
<<http://www.fhwa.dot.gov/pavement/asphalt/labs/mixtures/sgc.cfm>>.
18. Preparing and Determining the Density of Hot-Mix Asphalt (HMA) Specimens by Means of the Superpave Gyratory Compactor. AASHTO Designation: T312-04.
19. Troxler. “Gyratory Shear Kit”. June 16, 2009.  
<<http://www.troxlerlabs.com/PRODUCTS/gsk.shtml>>.
20. Ping, W., Yang, Z., Leonard, M., and Putcha, S. Laboratory Simulation of Field Compaction Characteristics on Sandy Soils. Transportation Research Board 81st Annual Meeting, Washington D.C., January 13-17, 2002.
21. Ping, W., Xing, G., Leonard, M., Yang, Z. Evaluation of Laboratory Compaction Techniques for Simulating Field Soil Compaction (Phase II). For the Florida Department of Transportation. 2003.
22. Mokwa, R., Cuelho, E., Browne, M. Laboratory Testing of Soil Using the Superpave Gyratory Compactor. Transportation Research Board 87th Annual Meeting, Washington D.C., January 13-17, 2008.
23. Donovan, P. and Tutumluer, E. (2008). Effect of Aircraft Load Wander on Unbound Aggregate Pavement Layer Stiffness and Deformation Behavior. Proceedings of the Airfield and Highway Pavements Conference, Bellevue, Washington, 2008.
24. Hayhoe, G. F., Garg, N. Consolidation of aggregate base and subbase layers under heavy aircraft loading at the National Airport Pavement Test Facility. Proceedings of the Advanced Characterisation of Pavements and Soil Engineering Materials, Athens, June 2007.

25. Archilla, A. R. Use of Superpave Gyratory Compaction Data for Rutting Prediction. *Journal of Transportation Engineering*, Vol. 132, No. 9, 2006, pp. 734-741.
26. National Airport Pavement Test Facility website, <<http://www.airporttech.tc.faa.gov/naptf/>>, Accessed July 30, 2009.
27. Garg, N. Gordon, G.F. Pavement Deformation Behavior of the Granular Layers Tested at the FAA's National Airport Pavement Test Facility. 3rd International Conference on Accelerated Pavement Testing, Madrid, October 2008.
28. Ping, W., Yang, Z., Leonard, M., and Putcha, S. Laboratory Simulation of Field Compaction Characteristics on Sandy Soils. Transportation Research Board 81st Annual Meeting, Washington D.C., January 13-17, 2002.
29. Mokwa, R., Cuelho, E., Browne, M. Laboratory Testing of Soil Using the Superpave Gyratory Compactor. Transportation Research Board 87th Annual Meeting, Washington D.C., January 13-17, 2008.
30. Lambert, N., Denny, K., Sukumaran, B., and Mehta, Y. Investigation of the performance of flexible airport pavements under moving aircraft wheel loads with wander using finite element analysis. ASCE Geotechnical Special Publication on Challenges and Recent Advances in Pavement Technologies and Transportation Geotechnics, GeoHunan, August 3-6, 2009.
31. Asphalt Institute Manual, SP-2 Superpave Mix Design 2001
32. 621IMG\_0077. Digital image. Seattle PI. Web. 22 Sept. 2009. <[http://www.seattlepi.com/dayart/20090922/621IMG\\_0077.JPG](http://www.seattlepi.com/dayart/20090922/621IMG_0077.JPG)>.
33. Airbus A380-38. Digital image. Aviation Spectator. Web. 14 Dec. 2011. <<http://www.aviationspectator.com/files/images/Airbus-A380-38.jpg>>.
34. Soil Compactor Roller Types. Digital image. Caterpillar Equipment. Web. 25 Jan. 2012. <[www.cat.com](http://www.cat.com)>.